Agricultural Water Management 243 (2021) 106473

Contents lists available at ScienceDirect

Agricultural Water Management

journal homepage: www.elsevier.com/locate/agwat

# Evapotranspiration partitioning and water productivity of rainfed maize under contrasting mulching conditions in Northwest China

Jing Zheng [a,b,c], Junliang Fan [a,*], Fucang Zhang [a], Qianlai Zhuang [b,c]

[a] Key Laboratory of Agricultural Soil and Water Engineering in Arid and Semiarid Areas of Ministry of Education, Northwest A&F University, Yangling 712100, China
[b] Department of Earth, Atmospheric and Planetary Sciences, Purdue University, West Lafayette, IN 47907, USA
[c] Department of Agronomy, Purdue University, West Lafayette, IN 47907, USA

ARTICLE INFO

*Keywords:*
Rainfed maize
Canopy interception
Soil evaporation
Plant transpiration
Water productivity

ABSTRACT

Soil mulching can effectively modify crop growth environments and increase crop productivity in rainfed agriculture, and the knowledge about water fluxes within the soil-crop-atmosphere ecosystem is essential for improving water productivity (WP) in water-limited regions such as Northwest China. This study systematically investigated seasonal and inter-annual dynamics of evapotranspiration (ET) partitioning into canopy interception ($I_c$), soil evaporation ($E_s$) and plant transpiration ($T_p$) in rainfed maize fields under four mulching conditions (NM: non-mulching, SM: straw mulching, RPBF: plastic-mulched ridge with bare furrow, and RPSF: plastic-mulched ridge with straw-mulched furrow) from June to October in 2015, 2016 and 2017 characterized by various seasonal rainfall distributions. The results showed that seasonal ET was slightly higher under mulching conditions compared with NM during each growing season, but the difference was not statistically significant. Soil mulching decreased $E_s$/ET (22.0–29.8 %, 14.3–19.5 % and 11.3–15.1 % under SM, RPBF and RPSF, respectively) relative to NM (27.6–34.5 %), while it increased $T_p$/ET (55.8–63.7 %, 63.0–71.0 % and 65.6–73.2 %, respectively) and $I_c$/ET (13.2–16.0 %, 14.7–17.4 % and 15.4–19.3 %, respectively) relative to NM (52.4–58.7 % and 13.0–15.7 %, respectively). Differences in ET partitioning under contrasting mulching conditions were related largely to variations in leaf area index and soil water stress. Although seasonal ET under various mulching conditions varied among the three seasons (264.8–286.6 mm in 2015, 241.2–242.5 mm in 2016 and 296.6–324.4 mm in 2017), the proportions of $I_c$ (13.0–15.4 %, 13.3–19.3 % and 15.7–17.7 %), $E_s$ (11.3–28.3 %, 15.1–34.5 % and 11.4–27.6 %) and $T_p$ (58.7–73.2 %, 52.4–65.6 % and 56.7–70.9 %) to total ET were similar. Soil mulching greatly enhanced maize yield by 9.5–26.1 %, 27.0–186.5 % and 30.8–209.7 % under SM, RPBF and RPSF compared with NM, respectively, resulting in 1.5–15.8 %, 19.0–184.7 % and 20.8–214.8 % higher WP, respectively. It was concluded that soil mulching largely promoted $T_p$ and restrained $E_s$ in spite of slight increase in $I_c$, thereby improving maize yield and WP during the three seasons. The present study gives a better understanding of rainwater cycle and crop water use, which is critical to sustainable management of rainfed agriculture.

## 1. Introduction

Evapotranspiration (ET) is a dominant component of hydrological cycle in agricultural systems, consisting of canopy interception ($I_c$), evaporation from soil surface ($E_s$) and transpiration by plants ($T_p$). $I_c$ is considered as the part of rainfall that is retained by crop canopy and finally returned to the atmosphere during and after rainfall (Fan et al., 2014), which is generally obtained by subtracting throughfall and stemflow from gross rainfall. Although some previous studies have shown that $I_c$ can absorb available energy which will evaporate the water residing on leaf surfaces in the farmland, or decrease the transpiration rate by increasing atmospheric water vapor content near the crop canopy and reducing the water pressure difference (Kraus, 1966; Stewart, 1977; Wang et al., 2007), it can decrease the availability of total rainwater input that reaches the soil surface, leading to great water losses in the agricultural ecosystem. Many studies on canopy rainfall interception have been conducted on crops, especially on maize plants, all of which clearly indicated that rainfall interception could not be ignored (Han et al., 2014; Zheng et al., 2018a, b). Therefore, it is essential to consider canopy interception loss separately from total ET.

* Corresponding author.
*E-mail address:* nwwfjl@163.com (J. Fan).

https://doi.org/10.1016/j.agwat.2020.106473
Received 3 March 2020; Received in revised form 3 June 2020; Accepted 21 August 2020

$E_s$ is another important part of the surface-water balance, but it does not enhance crop productivity. Micro-lysimeters have been widely used for determining $E_s$ from the bare soil in field experiments (Wang and Liu, 2007; Zhang et al., 2011; Anapalli et al., 2016; Consoli et al., 2017; Liu et al., 2018; Gonzalez-Dugo et al., 2019) and it is reported that about 20–30 % of growing-season ET participates in this water loss process for annual crops (Allen, 2011). $T_p$ refers to a substantial portion of ET through which soil water returns to the air from plant stomata, which is a contributing factor to crop yield. Heat balance-based sap flow probes are useful tools to measure plant water use, and many studies have suggested that they are suitable for estimating plant transpiration for small stems with low sap flow rates, e.g. maize plants (Zhang et al., 2016; Fan et al., 2018). Partitioning ET into $I_c$, $E_s$ and $T_p$ is desirable to improve the understanding of soil water loss processes and then to increase crop production through maximizing transpiration and reducing evaporation (Yimam et al., 2015).

Maize (*Zea mays L.*) is one of the major crops cultivated in summer in Northwest China (Huang et al., 2011). Soil water supplied by rainfall is the main factor that limits the physiological development and reproduction of rainfed maize in this region. It is therefore essential to conserve soil moisture and enhance crop water productivity (WP) by changing the balance of $I_c$, $E_s$ and $T_p$ through appropriate agronomic practices. Field management practices have been extensively applied to maintain crop production, especially plastic or straw mulching, which can efficiently improve soil water and temperature regimes and crop growth conditions (Li et al., 2013a, b; Liu et al., 2015; Li et al., 2017; Mo et al., 2018; Jia et al., 2018; Ding et al., 2018; 2019a; Zheng et al., 2020). However, the effects of various mulching patterns on ET remain inconsistent. Li et al. (2018) reported that mulching techniques (plastic film, gravel sand and straw) generally reduced total ET during the growth seasons of summer maize compared with non-mulching. However, Li et al. (2013a) concluded that the ridge and furrow mulching reduced ET at the early growth stage of spring maize, but increased ET at the middle growth stages and ET showed no obvious pattern at the later growth stage among different treatments. Thus, process-based investigation on the effects of mulching, especially water consumption mechanisms as a result of mulching, is important for improving WP in rainfed farming systems.

Soil mulching can modify the partitioning of ET into $I_c$, $E_s$ and $T_p$ by affecting soil moisture, soil temperature and subsequently maize growth. For instance, Zheng et al. (2018a, b) measured throughfall, stemflow, gross rainfall and further estimated $I_c$ of summer maize using the water balance method. They found that seasonal $I_c$ accounted for 7.4–21.4 % of gross rainfall under various mulching patterns and planting densities. Li et al. (2008) estimated maize ET and $E_s$ under plastic film-mulched condition at the Shiyanghe Station in Wuwei, Gansu Province of Northwest China by using eddy covariance and micro-lysimeters. They indicated that plastic mulching resulted in high $K_{cb}$ and low $K_e$, ranging from 0 to 1.2 and 0 to 0.3 over the whole season, which was related to plant growth and soil moisture. Gong et al. (2017) suggested that partial plastic mulching decreased average $E_s$/ET of rainfed maize by 11.2 % compared with non-mulching, and the ratio of $E_s$/ET changed as a logistic function of green leaf area index. Wang et al. (2019b) quantified the influence of plastic mulch on ET partitioning using an improved multisource energy balance model at Daman superstation located in Gansu Province of China. They found that mulching increased transpiration fraction and the effects of mulching on ET partitioning varied with leaf development. Feng et al. (2019) monitored ET on different time scales in non-mulched (CK) and plastic-mulched (PM) seed maize field in eastern Loess Plateau of China. They found that plastic mulching altered ET components, decreasing $E_s$/ET from 39.9–42.8 % under CK to 23.8–34.9 % under PM; it also increased $T_p$ by 9.8–33.3 % at the leaf scale and increased plant sap flow by 1.4–34.5 % compared with CK under contrasting climatic conditions.

Although previous studies have tried to quantify soil mulching effects on ET partitioning in rainfed maize fields, most of them mainly concentrated the flux separation under a specific mulching pattern, and few studies have investigated ET partitioning under various mulching conditions, particularly during maize growing seasons characterized by various temporal rainfall distributions. What's more importantly, issues related to ET partitioning into rainfall intercepted by canopies, vapour fluxes of plant transpiration and soil evaporation have been extensively studied for forested ecosystems (Raz-Yaseef et al., 2012; Fan et al., 2015; Benyon and Doody, 2015; Wang and Wang, 2017), but studies on maize ET partitioning have overlooked the effect of $I_c$, which reflects the influence of plants on the hydrological cycle in water-limited environments. To our knowledge, little attention has been paid to systematically determine the contributions of the three components ($I_c$, $E_s$ and $T_p$) to total ET in rainfed maize fields over the whole growing season under various mulching conditions. Therefore, the objectives of the present three-year study were to: (1) examine the seasonal and inter-annual variations of the three components of ET ($I_c$, $E_s$ and $T_p$) under various mulching patterns during the maize growing seasons of 2015, 2016 and 2017; (2) identify the main environmental and meteorological conditions influencing ET partitioning in this region; and (3) compare the influence of various mulching patterns on the contributions of $I_c$, $E_s$ and $T_p$ to total ET.

## 2. Materials and methods

### 2.1. Experimental site and design

The field experiments were performed during the maize growing seasons of 2015–2017 at the Key Laboratory of Agricultural Soil and Water Engineering in Arid and Semiarid Area of the Ministry of Education (34°18′N, 108°24 °E), Northwest A&F University, Northwest China. This region has a sub-humid but drought-prone climate, with an average annual sunshine hour over 2000 h, a mean annual temperature of 12.9 °C and a frost-free period over 210 d. The average annual precipitation during 1995–2014 is 560 mm (almost 65 % falling from June to September) and the average annual pan evaporation is 1500 mm. The soil is defined as a medium loam, which has a water holding capacity of 0.33 $cm^3$ $cm^{-3}$ and a permanent wilting point of 0.12 $cm^3$ $cm^{-3}$ for the topsoil (0–30 cm) (Gu et al., 2019). The groundwater table depth is more than 50 m and is not a feasible supplementary water source for maize growth.

Four mulching patterns replicated three times were studied in a randomized complete block design, i.e., non-mulching (NM), straw mulching (SM), ridge mulched with plastic film with bare furrow (RPBF), and plastic film-mulched ridge with straw-mulched furrow (RPSF). A schematic diagram showing various mulching patterns is illustrated in Fig. 1. The land area of each experimental plot was 15 $m^2$ (3 m × 5 m), and the plots were 1.5 m apart. Alternate ridges and furrows in RPBF and RPSF were shaped before maize seeds were sowed. The polyethylene plastic film was 80 cm in wide and 0.008 mm in thickness. Wheat straws harvested during the last season were cut into 15-cm-long pieces and spread on the soil surface under SM and in the furrow under RPSF at an application rate of 9000 kg $ha^{-1}$. The maize hybrid "Zhengdan958", a widely cultivated maize variety in this region, was planted at a population density of 67,500 plants $ha^{-1}$ (60 cm × 25 cm) on June 15th 2015, June 12th 2016 and June 14th 2017, and harvested on September 30th 2015, October 4th 2016 and October 6th 2017, respectively. All the fertilizers, i.e. Urea (N = 46 %, 180 kg $ha^{-1}$), calcium superphosphate ($P_2O_5$ = 16 %, 120 kg $ha^{-1}$) and potassium sulphate ($K_2O$ = 51 %, 60 kg $ha^{-1}$), were applied before maize planting. Irrigation was not applied over the whole maize growing seasons, and pest and weed control was performed as necessary.

### 2.2. Field measurements

#### 2.2.1. Leaf area index

Three plants per experimental plot were sampled to determine leaf

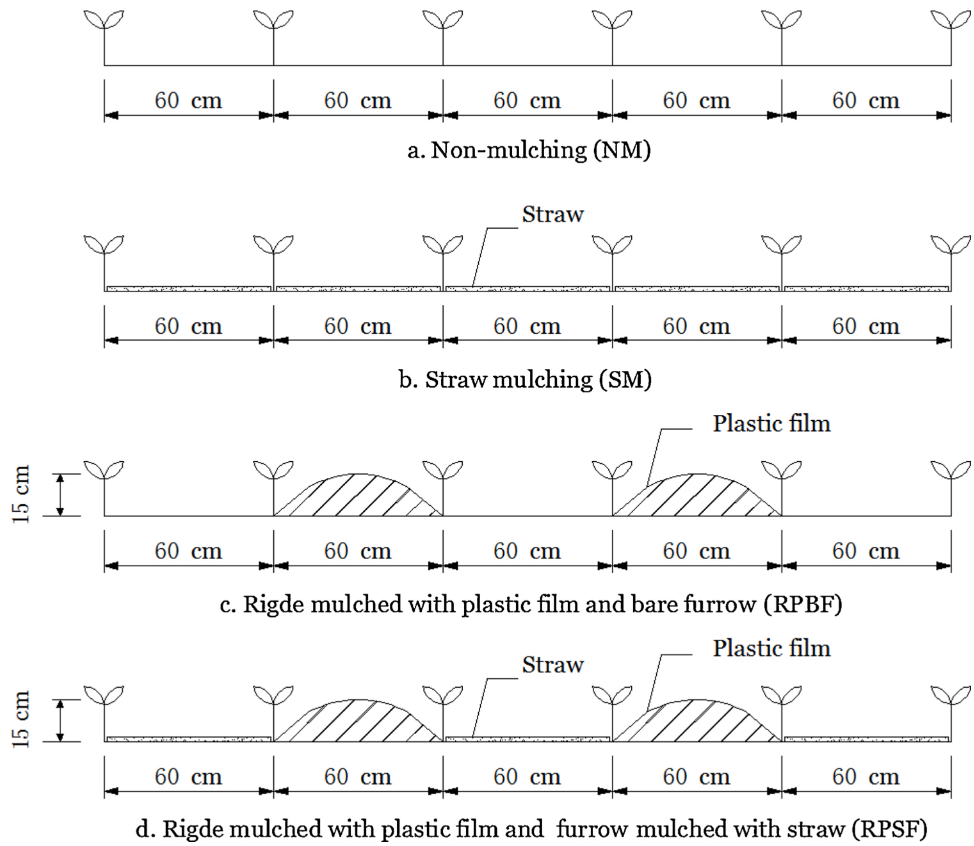


**Fig. 1.** Schematic diagram showing the configurations of the four mulching patterns.

length and leaf width at 5-10-day intervals. The area of each leaf was calculated by multiplying leaf length, width and a coefficient of 0.75 (Mckee, 1964). The leaf area of each plant was determined as the sum of each plant and its occupying land area (60 cm × 25 cm). Continuous LAI was obtained by fitting the equation proposed by Ding et al. (2013a):

$$\mathrm{LAI} = a \cdot DAS^{b} \cdot \exp(-r \cdot DAS) \quad (1)$$

where DAS is the days after sowing, r is the LAI change rate equal to 0.077 $m^2\ m^{-2}\ d^{-1}$, a and b are fitted coefficients. The entire growing season of summer maize was generally divided into four growth stages in the present study, including Seeding-Jointing (SJ), Jointing-Tasseling (JT), Tasseling-Grain filling (TG) and Grain filling-Maturity (GM). Each growth stage was further divided into earlier (I) and later (II) stages, i.e., SJ-I, SJ-II, JT-I, JT-II, TG-I, TG-II, GM-I and GM-II.

#### 2.2.2. Meteorological variables

During the three maize growing seasons, hourly climatic variables such as gross rainfall (GR), air temperature ($T_a$) and relative humidity (RH) were observed using a automatic weather station (Yangling National Meteorological Observing Station), which was installed 30 m away from the study plots. Ten-min averages of wind speed at 10 m were also obtained by the weather station ($u_{10}$). Wind speed obtained at the height of 10 m was further converted to speeds at the standard height of 2 m ($u_2$) using a logarithmic wind speed profile and conversion factor (Allen et al., 1998). Vapor pressure deficit (VPD) was determined from air temperature and humidity data following Campbell and Norman (1998). Solar radiation ($R_s$) was measured every hour with a Bowen ratio energy balance system (BREB) (Campbell Scientific Inc., USA) with a distance of 100 m. The FAO 56 Penman-Monteith formula was utilized for calculating daily reference evapotranspiration ($ET_0$) (Penman, 1948; Monteith, 1981; Allen et al., 1998).

#### 2.2.3. Canopy interception

Throughfall (TR) was collected using fifteen rainfall collectors under four neighboring maize plants at each experimental plot (Zheng et al., 2019). The depth of throughfall was then determined by the volume of collected rainwater dividing the cross-sectional area of throughfall collectors. Stemflow (S) was sampled on six maize plants with collars made by plastic plates, which were attached around the maize stems. Stemflow water in collars was drained to collectors using a slot with a transfer hose (Lamm and Manges, 2000). The depth of stemflow was determined as the ratio of stemflow volume and stemflow catchment area (60 cm × 25 cm). The detailed measurements of TR and S can be found in Zheng et al. (2019). $I_c$ was calculated as the difference between GR, TR and S as follows:

$$I_C = GR - TR - S \quad (2)$$

In addition, relative canopy interception (%) was defined as the ratio of $I_c$ to gross rainfall.

#### 2.2.4. Soil evaporation and sap flow rate

Soil evaporation ($E_s$) was observed by micro-lysimeters made from PVC pipes with a height of 20 cm and a diameter of 10.5 cm (Boast and Robertson, 1982). Two ML cylinders were installed at each plot. For flat cultivation, one was installed in the planting row and the other in between two neighboring rows. For cultivation with ridge and furrow, one was located on the ridge and the other in the furrow. The micro-lysimeters were changed and refilled with undisturbed soil samples every seven days or within one day following heavy rainfall (>5 mm $day^{-1}$) (Liu et al., 2012; Balwinder-Singh et al., 2016; Wang and Wang, 2017). Daily $E_s$ was calculated as the difference in micro-lysimeter weight between the beginning and ending points of the day (18:00 pm). Soil evaporation could not be measured on rainy days due to the influence of rainfall over the micro-lysimeters, so we assumed that soil evaporation was zero on rainy days in this study similar to Wang and

Wang (2017).

The heat balance-based Dynagage Flow32−1 K system (Model SGA5/9/13/19/25-WS, Dynamax, Houston, TX, USA) was used to measure sap flow rates (Jiang et al., 2016). The sensors were installed on three maize stems in each mulching treatment (one sensor per each plot) after July 1. The sensors were insulated with silica gel and aluminum foil for minimizing energy exchange and preventing from rainfall. The sensors were moved to various maize plants every 10–15 days to minimize maize damage from high temperatures of sap flow sensors. The sensors output was measured at 60 s intervals and recorded every 30 min as the average value. The measured sap flow rate was corrected using the calibration equation of Wang et al., 2017. The hourly sap flow rate for each maize plant under various mulching patterns was then calculated as the average sap flow rate for the three sample plants ($Q_h$, g $h^{-1}$ $plant^{-1}$). The daily plant water use was the sum of $Q_h$ in a day ($Q_d$, L $day^{-1}$ $plant^{-1}$). Maize plant water use ($Q_d$, L $day^{-1}$ $plant^{-1}$) was then upscaled to $T_P$ (mm $d^{-1}$) using the following equation:

$$T_P = Q_d / A \quad (3)$$

where A is the average ground area occupied by a maize plant ($m^2$).

#### 2.2.5. Soil water content

Fine roots of summer maize are mainly concentrated within the 0−60 cm soil profile (Liu et al., 2017). Soil water content was thus measured using calibrated $ECH_2O$-5TE sensors (Decagon Devices, Inc., Pullman, WA, USA) at 10, 20, 30 and 50 cm depths. Data were recorded at 15 min intervals by data loggers and daily average SWC was calculated by averaging 15-min values. Two sets of sensors were installed under NM and SM, one in the maize row and the other in between two neighboring rows. Three sets of sensors were used under RPBF and RPSF, which were installed in between two furrows, in between two ridges and at the boundary of two neighboring ridge and furrow, respectively. Averaged daily soil moisture in the top 50 cm soil layer was calculated by averaging observed SWC at different soil depths and locations for further data analyses. Gravimetric soil water content was also measured in the 0–20, 20–40, 40–60, 60–80, 80–100, 100–125, 125–150 cm soil layers before sowing and after harvesting to calculate changes in soil water storage throughout the growing seasons and then obtain WP of maize. Volumetric water content was attained by multiplying gravimetric water content and dry bulk density obtained from oven-dried weights (dried at 105 °C).

#### 2.2.6. Grain yield and water productivity

The grain yield of maize was determined after harvest at a 12.5 % moisture based on the four central rows of the plots excluding two plants at the row ends. Seasonal ET was obtained from two approaches, i.e., soil water balance method ($ET_{WB}$) and the sum of $I_c$, $E_s$ and $T_P$ ($ET_{IET}$). Seasonal $ET_{WB}$ was obtained using the equation $ET_{WB}$ =GR+ΔS, where GR is the gross rainfall over the maize growing season and ΔS is the change in soil water storage in the 150 cm soil profile. No surface runoff was considered as a result of the flat land surface and the deep percolation was also neglected considering the small rainfall input to the soil and large soil water-holding capability. Seasonal $ET_{ISP}$ was determined by summing canopy interception ($I_c$), $E_s$ from ML and $T_P$ from sap flow, i.e., $ET_{ISP} = I_c + E_s + T_P$. WP was determined as the ratio of grain yield (GY) and $ET_{ISP}$, i.e., WP = GY/ $ET_{ISP}$.

### 2.3. Data analysis

The path analysis method was employed to assess the relationships between y ($E_s$: daily soil evaporation and $T_P$: daily plant transpiration) and x ($R_s$, $T_a$, VPD, RH, $u_2$, LAI and SWC) using the SPSS 16.0 software (SPSS Inc., Chicago, USA). Only 234 days of $E_s$ data and influencing factors were used for path analysis in Table 2 due to rainy days. The SPSS software was also used for statistical analysis and regressions. One-way ANOVA analysis (significant at the $P < 0.05$ level) was used to test the statistical differences of maize yield, the ratios of $I_c$, $E_s$ and $T_P$ to total ET and WP among different mulching patterns. All of the figures were plotted using Sigmaplot 10.0 (Systat Software, San Jose, CA).

## 3. Results

### 3.1. Environmental conditions and leaf area index

Dynamics of daily climatic parameters during the growing seasons of summer maize from 2015 to 2017 are presented in Fig. 2. Average daily $R_s$ during the three seasons were 203.24, 209.62 and 217.44 W $m^{-2}$, respectively. Average $T_a$ and VPD were slightly higher in 2016 (25.6℃, 0.94 K Pa) than those in 2015 (24.2℃, 1.07 K Pa) and 2017 (24.8℃, 1.05 K Pa). However, average RH was slightly higher in 2015 (71.1 %) and 2017 (70.8 %) than that in 2016 (69.3 %). Wind speed ($u_2$) ranged 0.3-2.5, 0.5-4.1 and 0.5-3.1 m $s^{-1}$ during the three seasons, respectively. Total $ET_0$ were 413.0, 483.1 and 472.3 mm during the three seasons, respectively. Fig. 3 presents the trends in rainfall and averaged volumetric soil water content (SWC) (0−50 cm) during the three seasons. Gross rainfall was 269.9, 261.1 and 287.4 mm during the growing seasons of 2015, 2016 and 2017, respectively. Although similar total rainfall amount was observed, the seasonal temporal rainfall distribution differed greatly. In 2015, rainfall distributed at the four growth stages accounted for 31.4 %, 15.6 %, 23.0 % and 30.0 %, respectively. However, only 4.4 % of total rainfall was spread from tasseling to grain filling stage in 2016 and 7.1 % from seedling to jointing stage in 2017. SWC under all treatments showed similar trends, but SWC with soil mulching was generally higher than that of non-mulching. Seasonal average SWC under NM, SM, RPBF and RPSF was 23.1 %, 23.7 %, 23.4 % and 23.2 % in 2015, 20.4 %, 21.2 %, 21.9 % and 22.0 % in 2016, and 22.1 %, 22.9 %, 23.3 % and 23.4 % in 2017. Long intervals between rainfall events in August 2016 allowed SWC to dramatically decline (Fig. 3). As maize grew, leaf area index (LAI) increased rapidly after 40 DAS and obtained the maximum value 60–70 DAS, with maximal LAI of 3.56 (NM), 4.14 (SM), 4.42 (RPBF) and 5.09 (RPSF) $m^2$ $m^{-2}$ in 2015, 5.33 (NM), 5.58 (SM), 6.00 (RPBF) and 6.24 (RPSF) $m^2$ $m^{-2}$ in 2016, and 3.46 (NM), 4.11 (SM), 4.60 (RPBF) and 5.00 (RPSF) $m^2$ $m^{-2}$ in 2017 (Fig. 4). LAI declined after 70 DAS during the three seasons, and the decrease in LAI at the late growth stage of 2016 was larger than those in 2015 and 2017 (Fig. 3).

### 3.2. Canopy interception and its influencing factors

Number of rainfall events, rainfall depth and canopy interception ($I_c$) under various mulching patterns at each maize growth stage in 2015, 2016 and 2017 are shown in Table 1. Total growing-season canopy interception was 34.37, 37.66, 41.48 and 44.24 mm, 32.01, 34.96, 42.28 and 45.82 mm, and 46.44, 51.75, 54.58 and 57.56 mm under NM, SM, RPBF and RPSF in 2015, 2016 and 2017, respectively. It was always in the order of NM < SM < RPBF < RPSF during the three growing seasons, although there was no significant difference among various mulching patterns in 2015 and 2017. Canopy interception at various growth stages was similar to the variation of growing-season canopy interception, which was always lower under NM and higher under RPSF.

Generally, $I_c$ increased with increasing gross rainfall (GR) amount under all mulching patterns during 2015–2017 (Fig. 4). At the seedling to jointing stage, $I_c$ showed weaker relationships with GR than those at the other stages, which was mainly resulted from the much smaller LAI at this growth stage. $I_c$ was higher under soil mulching when GR was the same. The relative canopy interception generally decreased with increasing rainfall amount, and tended to be constant for larger rainfall events. These power regression lines also showed that $I_c$ was in the order of NM < SM < RPBF < RPFS, which was mainly due to the differences in LAI among the four mulching conditions. The relationship between canopy interception amount and LAI was not obvious among the four

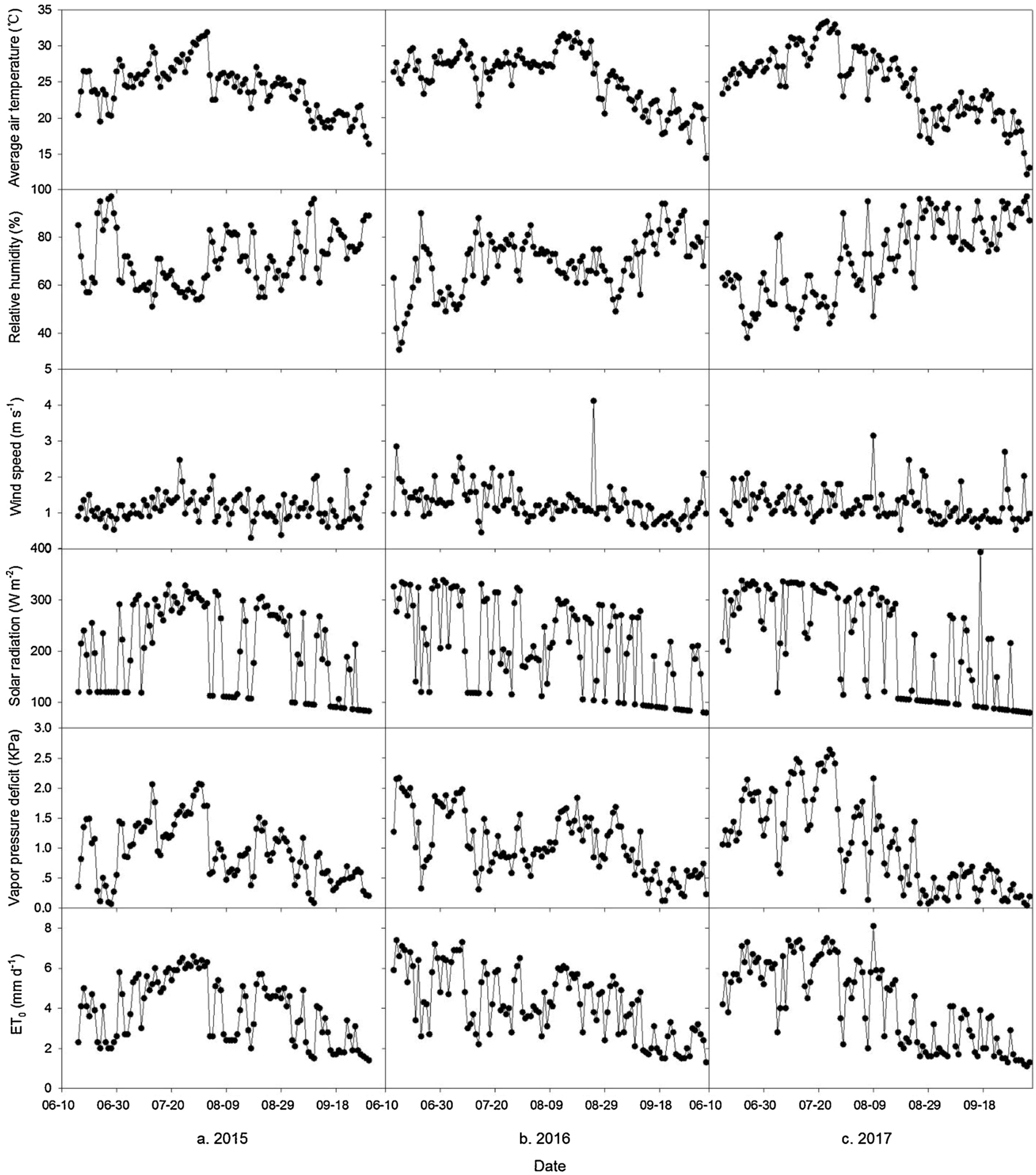


**Fig. 2.** Seasonal variations of meteorological variables and reference evapotranspiration ($ET_0$) during the three maize growing seasons of 2015–2017.

mulching patterns at different rainfall classes during 2015–2017 (Fig. 5). However, obvious positive power correlations were found between the relative canopy interception and LAI ($R^2 > 0.66$) for all rainfall events. These fitted equations were similar under NM, SM, RPBF and RPSF, confirming that soil mulching enhanced canopy interception by directly increasing LAI.

### *3.3. Soil evaporation dynamics*

The dynamics of soil evaporation during the growing seasons of 2015–2017 are shown in Fig. 6. Daily soil evaporation varied over the experimental periods, which showed a relatively high daily evaporation rate of 0.68 mm $d^{-1}$ from seedling to tasseling and dropped at the end of the tasseling stage to 0.36 mm $d^{-1}$ from tasseling to maturity. Soil mulching can significantly restrain the soil evaporation. Daily soil evaporation was always higher under NM and lower under RPSF during the three growing seasons. Maximum daily soil evaporation was 2.47, 2.32 and 2.12 mm $d^{-1}$ under NM, 2.09, 1.90 and 1.95 mm $d^{-1}$ under SM, 1.41, 1.39 and 1.22 mm $d^{-1}$ under RPBF and 1.28, 1.16 and 1.02 mm $d^{-1}$ under RPSF in 2015, 2016 and 2017, respectively. Daily mean soil evaporation under NM, SM, RPBF and RPSF was 0.71, 0.62, 0.38 and 0.31 mm $d^{-1}$ in 2015, 0.76, 0.66, 0.43 and 0.33 mm $d^{-1}$ in 2016, 0.73, 0.63, 0.42 and 0.33 mm $d^{-1}$ in 2017, respectively. The seasonal total soil evaporation under NM, SM, RPBF and RPSF was 74.9, 66.2, 40.4 and 32.5 mm in 2015, 82.9, 72.0, 47.4 and 35.8 mm in 2016, and 81.9, 71.0, 47.5 and 36.8 mm in 2017, respectively.

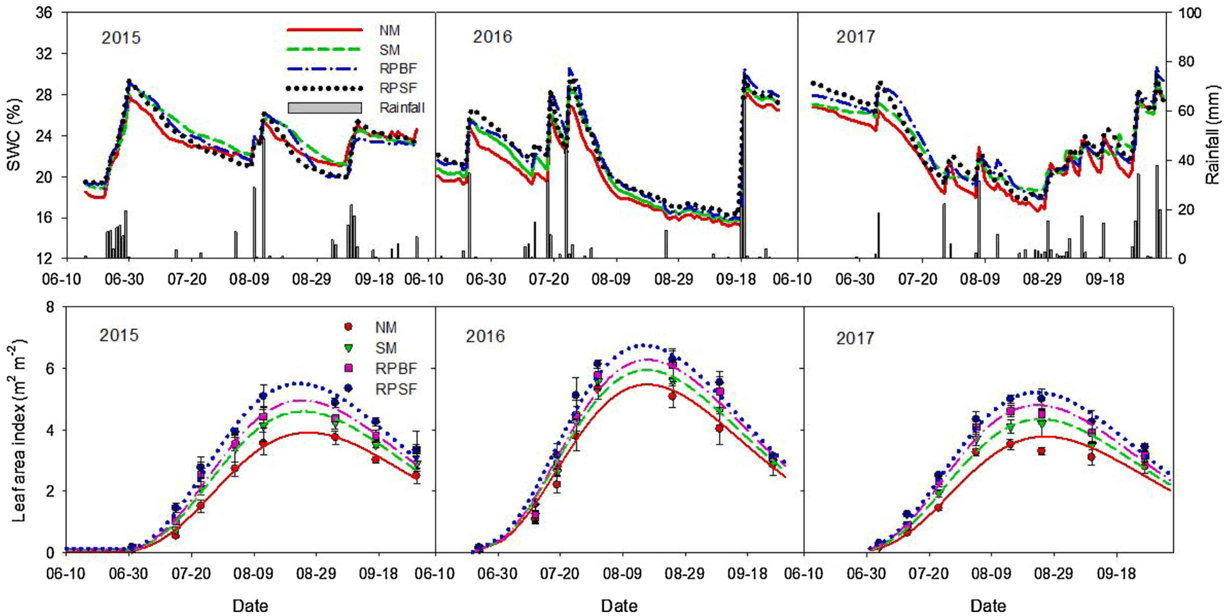


**Fig. 3.** Seasonal variations of volumetric soil water content (SWC) (0−50 cm) and leaf area index under various mulching patterns during the three maize growing seasons of 2015–2017.

### 3.4. Plant transpiration dynamics

Fig. 7 presents the diurnal variation of sap flow rate during the representative sunny, cloudy and rainy days under the four mulching patterns in 2017. Sap flow rate had an obvious day-night rhythm synchronous with solar radiation. On sunny days (August 5 and August 9–12), maize sap flow rate enhanced to mid-day and then declined, with the mean sap flow rates of 29.5, 35.0, 37.4 and 40.5 g $h^{-1}$ under NM, SM, RPBF and RPSF, respectively. However, it slightly decreased around 14:00 and then recovered, which was extremely obvious on August 9-10. There were 2.4, 31.7 and 0.1 mm rainfalls from August 6–8, respectively, causing lower sap flow on these days. Nevertheless, fluxes obviously increased after rain cessation compared to fluxes on August 5 (sunny day), and reached higher values on August 9 then decreased with the soil drying. On rainy and cloudy days (August 6–7 and August 18–22), $R_s$ had a wide range of fluctuations, and sap flow rate also showed fluctuating increase-decrease trends, with average sap flow rates of 8.1, 10.1, 11.0 and 11.6 g $h^{-1}$ under NM, SM, RPBF and RPSF, respectively.

Daily plant transpiration varied over the experimental periods, which increased rapidly from seedling with average value of 1.52 mm $d^{-1}$, kept at higher values (2.65 mm $d^{-1}$) at the middle stage, and decreased gradually at the later stage (0.88 mm $d^{-1}$) during the three seasons, having similar variations with ET (Fig. 1, Fig. 8). The maximum daily transpiration of summer maize appeared on 22 August in 2015, 29 July in 2016 and 9 August in 2017, with values of 4.38, 5.26 and 6.62 mm $d^{-1}$ under NM, 5.11, 5.69 and 6.83 mm $d^{-1}$ under SM, 5.34, 5.95 and 8.38 mm $d^{-1}$ under RPBF and 5.39, 6.01, 8.62 mm $d^{-1}$ under RPSF in 2015, 2016 and 2017, respectively. The cumulative water consumption through plant transpiration was significantly enhanced by soil mulching. Total plant transpiration under NM, SM, RPBF and RPSF treatment were 155.50, 181.86, 200.58 and 209.95 mm in 2015, 126.68, 134.94, 152.91 and 155.53 mm in 2016, and 168.30, 200.43, 220.96 and 230.04 mm in 2017, respectively. It should be noted that the difference in daily plant transpiration among the four mulching modes was larger at the middle stage than that at the earlier and later stages.

### 3.5. Controlling factors of $E_s$ and $T_P$

Fig. 9 presents relationships between daily $E_s$, $T_P$ against $ET_0$ under various mulching patterns during 2015–2017. There were positive correlations between $E_s$, $T_P$ and $ET_0$ during the three seasons ($P < 0.001$). $ET_0$ was directly affected by meteorological variables. Therefore, $R_s$, $T_a$, VPD, RH, $u_2$, LAI and SWC were selected to analyze the controlling factors of soil evaporation ($E_s$) and plant transpiration ($T_P$) using the path analysis method. With regard to the correlation between each factor to $E_s$, the highest correlation was observed for $R_s$ (0.499), followed by RH (-0.400), VPD (0.398), LAI (-0.398), $T_a$ (0.337), $u_2$ (0.301) and SWC (0.170), where the coefficients of determination were 0.213, 0.090, -0.239, 0.152, 0.117, 0.039 and -0.013, respectively. The effects of all these factors on $E_s$ were extremely significant ($P_{ij}<0.001$) (Table 2). The direct coefficients between $R_s$, $T_a$, VPD, RH, $u_2$, LAI as well as SWC and $E_s$ were 0.426, 0.347, -0.601, -0.224, 0.131, -0.381 and -0.074, respectively. VPD had very high positive indirect effect through $R_s$, $T_a$ and RH (0.999), and SWC had high positive indirect effect through LAI (0.244). As for $T_P$, higher correlations were observed for $R_s$, $T_a$, VPD and RH (0.659, 0.536, 0.517 and -0.498, respectively), and lower correlations for $u_2$, LAI and SWC (0.085, 0.119 and -0.032, respectively), with no significant influence of SWC ($P = 0.143$). The coefficients of determination for $T_P$ based on $R_s$, $T_a$, VPD, RH, $u_2$, LAI and SWC were 0.385, 0.132, -0.044, 0.041. 0.002. 0.049 and -0.008, respectively. The direct coefficients were 0.584, 0.246, -0.086, -0.083, 0.025, 0.408 and 0.235, respectively. The direct coefficient of VPD, RH and $u_2$ were not significant ($P > 0.05$), but the indirect effects of VPD and RH on $T_P$ through $R_s$ were high (0.447 and -0.447, respectively). Under various mulching conditions, LAI and SWC were responsible for the difference of $E_s$ and $T_P$ because of the same climatic conditions during the experimental periods, in which the influence of LAI was higher than SWC and the influence of SWC was more complex ($b_i$=-0.074, $P_i$<0.05, $r_{ij}$ = 0.170, $P_{ij}$<0.001 for $E_s$; $b_i$ = 0.235, $P_i$<0.001, $r_{ij}$=-0.032, $P_{ij}$>0.05 for $T_P$).

### 3.6. Variations in proportions of $I_c$, $E_s$ and $T_P$ to total ET

The ratios of $I_c$, $E_s$ and $T_P$ to total ET differed among the four mulching patterns during the maize growing seasons of 2015–2017 (Table 3, Fig. 10). The variation of $T_P$/ET displayed a strong seasonal pattern. It increased continuously at the early growth stage, and became relatively constant from jointing to grain filling, and then experienced a decrease after grain filling. At most growth stages, the contribution of $T_P$

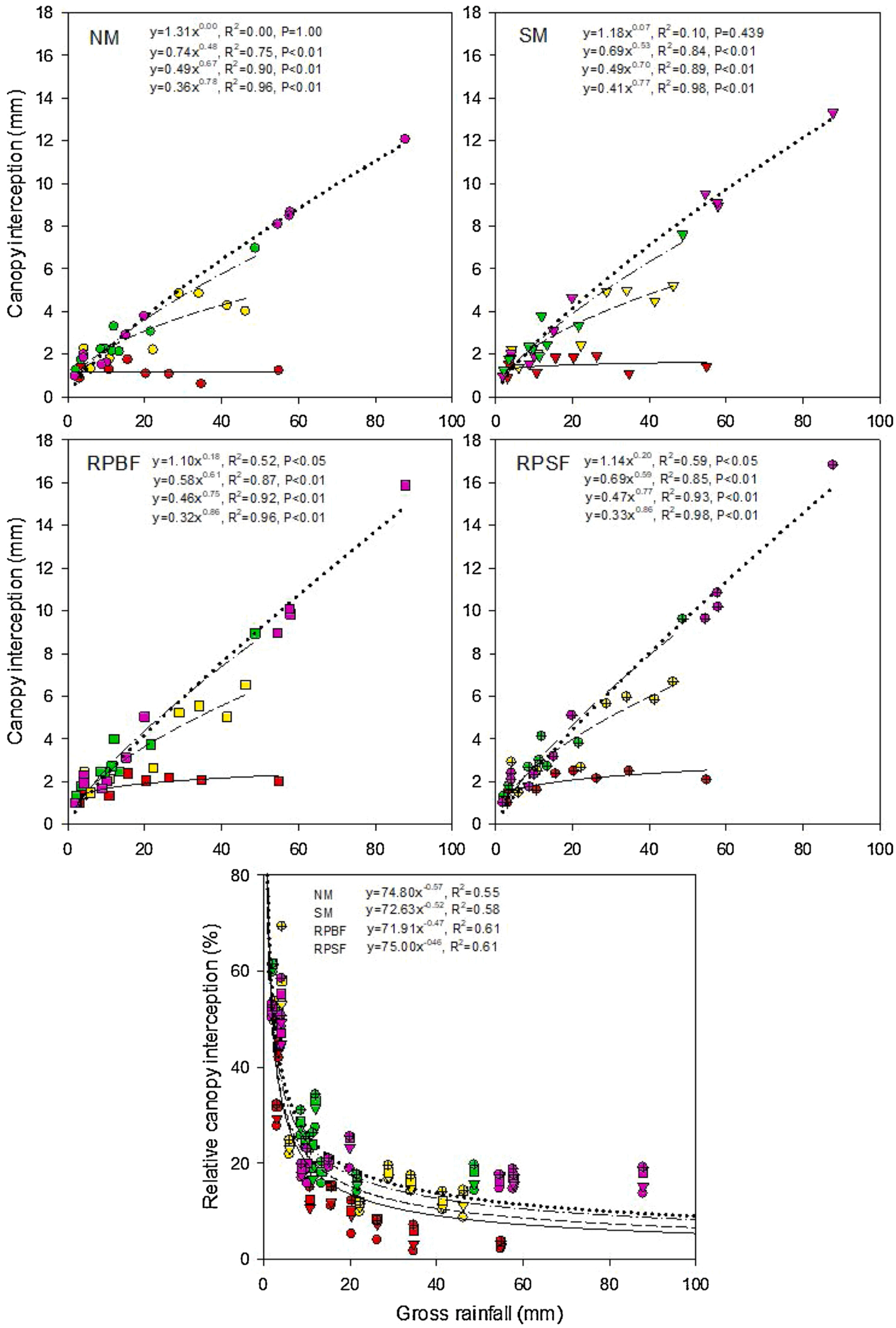


**Fig. 4.** Relationship between canopy interception and gross rainfall under various mulching patterns of summer maize during 2015–2017. Red: seedling to jointing; Yellow: jointing to tasseling; Green: tasseling to grain filling; Pink: grain filling to maturity.

to total ET was significantly enhanced by soil mulching. $E_s$/ET showed an opposite trend to $T_P$/ET in 2015 and 2017, which decreased from late June to August, stabilized at low level and increased slightly at the late growth stage. The value of $E_s$/ET was nearly zero at the TG-II stage in 2017 due to continuous rainfall from August 25th to September 5th. In addition, $E_s$/ET from jointing to grain filling in 2016 was different from those during the other two seasons at the same growth stage, maintaining relatively high level. The variation of $I_c$/ET had no obvious consistent pattern and the contribution of $I_c$ to ET showed almost no significant difference among various mulching conditions throughout the three seasons. During the whole growing season, $E_s$ was always in the order of RPSF < RPBF < SM < NM, ranging from 11.3% to 34.4% under various mulching patterns during 2015–2017 (Table 3). $I_c$ was the smallest component, ranging from 13.0% to 19.3% during the three seasons. $T_P$ represented the greatest proportion of ET, ranging from 52.4% to 73.2%. The ratios of $I_c$ and $T_P$ to ET were largest under RPSF, followed by RPBF, SM and NM.

### 3.7. Grain yield and water productivity

Among the three growing seasons, grain yield and ET were 1366.9-9073.9 kg ha$^{-1}$ and 237.13–324.44 mm in various mulching

**Table 1**
Number of rainfall events, gross rainfall and canopy interception ($I_c$) at various growth stages of summer maize under the four mulching patterns during 2015–2017.

| Mulching pattern | | 2015 | | | | | 2016 | | | | | 2017 | | | | |
|---|---|---|---|---|---|---|---|---|---|---|---|---|---|---|---|---|
| | | Seeding-Jointing | Jointing-Tasseling | Tasseling-Grain filling | Gain filling-Maturity | Total | Seeding-Jointing | Jointing-Tasseling | Tasseling-Grain filling | Gain filling-Maturity | Total | Seeding-Jointing | Jointing-Tasseling | Tasseling-Grain filling | Gain filling-Maturity | Total |
| | Number of rains | 3 | 3 | 2 | 4 | 12 | 4 | 3 | 1 | 3 | 11 | 1 | 3 | 6 | 4 | 14 |
| | Gross rainfall (mm) | 84.7 | 42.2 | 62.1 | 80.9 | 269.9 | 64.1 | 91.8 | 11.4 | 93.8 | 261.1 | 20.3 | 62.3 | 57.5 | 89.6 | 287.4 |
| NM | $I_c$ (mm) | 3.76a | 7.80a | 9.07a | 13.74a | 34.37a | 4.47a | 10.54b | 1.91a | 14.85b | 32.01b | 1.08a | 8.35a | 13.79a | 23.23b | 46.44a |
| SM | $I_c$ (mm) | 4.88a | 8.29a | 10.06a | 14.43a | 37.66a | 5.50a | 11.93b | 2.15a | 16.12ab | 34.96ab | 1.85a | 8.80a | 14.78a | 26.33a | 51.75a |
| RPBF | $I_c$ (mm) | 5.74a | 8.56a | 11.40a | 15.78a | 41.48a | 6.75a | 14.01a | 2.72a | 18.80ab | 42.28ab | 2.04a | 9.65a | 15.70a | 27.19a | 54.58a |
| RPSF | $I_c$ (mm) | 5.80a | 9.45a | 12.33a | 16.66a | 44.24a | 7.47a | 15.43a | 3.00a | 19.92a | 45.82a | 2.49a | 10.12a | 16.19a | 28.75a | 57.56a |

treatments, respectively (Table 3). There were significant differences in GY among mulching treatments, but ET was not significantly affected. Compared with NM, soil mulching increased grain yield by 138.5-2999.0 kg $ha^{-1}$ and ET by -4.0–27.8 mm. Water productivity (WP) under NM, SM, RPBF and RPSF were 22.42, 22.75, 26.69, and 27.08 kg $ha^{-1}$ $mm^{-1}$ in 2015, 5.67, 6.22, 16.14 and 17.85 kg $ha^{-1}$ $mm^{-1}$ in 2016, and 20.48, 23.71, 26.76 and 27.97 kg $ha^{-1}$ $mm^{-1}$ in 2017, respectively. It can be found that $ET_{ISP}$ were higher than $ET_{WB}$ by 23.29–37.27 mm in 2015, by 20.75–32.87 mm in 2016 and by 38.02–43.18 mm in 2017, with relative error of 9.3 %–15.3 % in 2015, 9.4 %–16.1 % in 2016 and 13.3 %–15.9 % in 2017. This indicated that ET values obtained from throughfall, stemflow, micro-lysimeter and sap flow measurements were comparable to those from the water balance method.

## 4. Discussion

### *4.1. Canopy interception*

Growing-season $I_c$ was in the order of NM < SM < RPBF < RPSF due to the good growth conditions when applying soil mulching. Gross rainfall firstly arrives leaf surfaces, and part of rainfall is intercepted and returns back to the air through evaporation. Therefore, leaf area is a significant factor affecting canopy interception. A positive relationship between canopy interception and maize LAI was found in this study, which agrees well with the finding of Zheng et al. (2012). Compared with NM, there was more water available under straw and plastic film mulching (Fig. 3), which promoted maize growth and development in rainfed regions and resulted in greater LAI and subsequently canopy interception. When LAI was large, the increasing rate of relative canopy interception slowed down since the leaf overlapping slowed increasing canopy coverage. Maize canopy interception accounted for 12.3–20.0 % of gross rainfall during 2015–2017 in this study, which was higher than those reported previously (7.5–13.3 %) (Lin et al., 2011; Han et al., 2014; Zheng et al., 2012). This can be attributed to the much higher LAI in our study as a result of higher planting density, compared with previous studies $LAI_{max}$ = 2.2-3.2 $m^2$ $m^{-2}$). Canopy interception also depends on meteorological factors, especially rainfall characteristics. Our results showed that $I_c$ increased slowly and gradually stabilized as GR continued to increase, suggesting that maize canopy was gradually saturated. With regard to the fitting relation between $I_c$ and GR, power function seemed to the most reasonable, which agrees with the findings of Yan et al. (2005) and Li et al. (2009). The percentage of canopy interception first decreased sharply and then began to be stable with increasing GR, implying that larger canopy interception would occur during small rainfall events (Zhang et al., 2015). This also indicated that canopy attained its maximum evaporation loss during rainfall with increasing GR and after saturation of canopy. Zhang et al. (2015) also revealed that the percentage of $I_c$ decreased with the increase if rainfall intensity. In the semi-humid but drought-prone region, rainfall intensity was generally smaller than that under artificially rainfall conditions (Han et al., 2014), leading to great rainfall interception and evaporation in our study.

### *4.2. Soil evaporation*

Growing-season soil evaporation decreased with varying degrees when covered with wheat straw or plastic film on the soil surface. In the present study, the path analysis showed that $E_s$ was significantly affected by all the investigated factors in spite of low correlation in SWC (Table 2). The climatic conditions were the same in the four mulching treatments, so LAI and SWC were mainly responsible for the difference in soil evaporation. Our results showed that positive relationship existed between daily $E_s$ and SWC ($r_{ij}$ = 0.170, $P_{ij}$<0.001) during the three growing seasons of summer maize. However, $b_i$ based on SWC was -0.074, with $P_i$ of = 0.026 (<0.005) further reflecting the complex mechanism of SWC on $E_s$. For instance, although soil mulching improved

**Table 2**
Path analysis between soil evaporation ($E_S$), plant transpiration ($T_p$) and each environmental variable and leaf area index (LAI) for all mulching patterns during 2015–2017.

| | Variables | $b_i$ | $r_{ij}b_j$ | | | | | | | | $r_{iy}$ | $R_i^2$ | $P_i$ | $P_{ij}$ |
|---|---|---|---|---|---|---|---|---|---|---|---|---|---|---|
| | | | | $R_s$ | $T_a$ | VPD | RH | $u_2$ | LAI | SWC | | | | |
| $E_S$ | $R_S$ | 0.426 | 0.073 | | 0.196 | −0.404 | 0.146 | 0.040 | 0.105 | −0.010 | 0.499 | 0.213 | 0.000** | 0.000** |
| | Ta | 0.347 | −0.010 | 0.241 | | −0.496 | 0.135 | 0.054 | 0.053 | 0.003 | 0.337 | 0.117 | 0.000** | 0.000** |
| | VPD | −0.601 | 0.999 | 0.286 | 0.287 | | 0.208 | 0.066 | 0.157 | −0.005 | 0.398 | −0.239 | 0.000** | 0.000** |
| | RH | −0.224 | −0.176 | −0.278 | −0.210 | 0.557 | | −0.065 | −0.188 | 0.007 | −0.400 | 0.090 | 0.050* | 0.000** |
| | $u_2$ | 0.131 | 0.170 | 0.131 | 0.143 | −0.305 | 0.111 | | 0.092 | −0.002 | 0.301 | 0.039 | 0.000** | 0.000** |
| | LAI | −0.381 | −0.017 | −0.117 | −0.048 | 0.248 | −0.111 | −0.032 | | 0.041 | −0.398 | 0.152 | 0.000** | 0.000** |
| | SWC | −0.074 | 0.244 | 0.060 | −0.016 | −0.037 | 0.022 | 0.003 | 0.212 | | 0.170 | −0.013 | 0.026* | 0.000** |
| | e | | | | | | | | | | | 0.642 | | |
| $T_p$ | $R_s$ | 0.584 | 0.075 | | 0.163 | −0.066 | 0.064 | 0.002 | −0.088 | 0.000 | 0.659 | 0.385 | 0.000** | 0.000** |
| | $T_a$ | 0.246 | 0.290 | 0.388 | | −0.075 | 0.062 | 0.006 | −0.053 | −0.039 | 0.536 | 0.132 | 0.000** | 0.000** |
| | VPD | −0.086 | 0.603 | 0.447 | 0.213 | | 0.079 | 0.006 | −0.125 | −0.017 | 0.517 | −0.044 | 0.389 | 0.000** |
| | RH | −0.083 | −0.415 | −0.447 | −0.184 | 0.082 | | −0.005 | 0.124 | 0.016 | −0.498 | 0.041 | 0.265 | 0.000** |
| | $u_2$ | 0.025 | 0.060 | 0.054 | 0.060 | −0.020 | 0.016 | | −0.037 | −0.012 | 0.085 | 0.002 | 0.229 | 0.002** |
| | LAI | 0.408 | −0.289 | −0.127 | −0.032 | 0.026 | −0.025 | −0.002 | | −0.130 | 0.119 | 0.049 | 0.000** | 0.000** |
| | SWC | 0.235 | −0.267 | 0.000 | −0.041 | 0.006 | −0.006 | −0.001 | −0.225 | | −0.032 | −0.008 | 0.000** | 0.143 |
| | e | | | | | | | | | | | 0.443 | | |

Note: $b_i$, $r_{ij}b_j$, $r_{iy}$, $R_i^2$, $P_i$ and $P_{ij}$ are the direct path coefficients, indirect path coefficients, correlation coefficients, coefficients of determination, significance of the direct path coefficients and significance of the correlation coefficients, respectively. e is the error term.

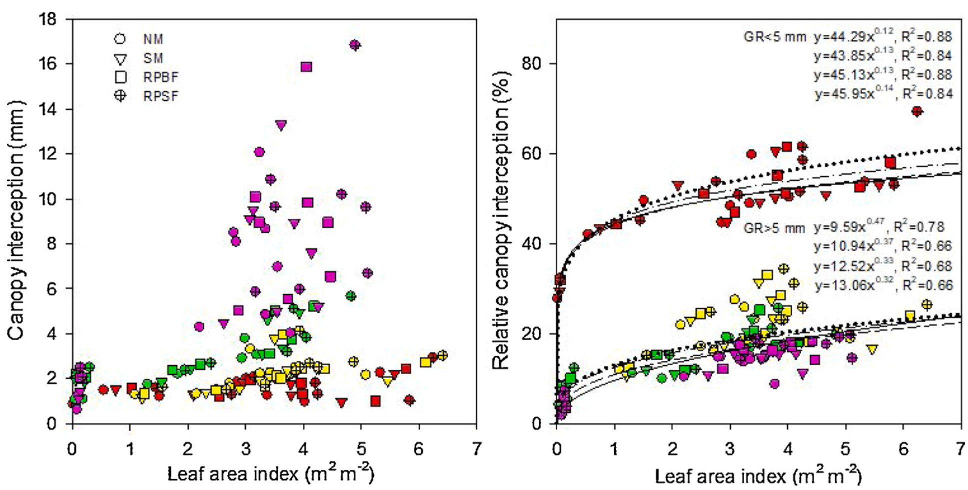


**Fig. 5.** Relationship between canopy interception and leaf area index for summer maize under various mulching patterns during 2015–2017. Red: 0−5 mm; Yellow: 5−15 mm; Green: 15−30 mm; Pink: > 30 mm.

soil water condition, lower soil evaporation was observed with mulching. Li et al. (2013b) indicated that straw mulching as a barrier reduced the rate of water flux changed from liquid to vapor forms from the soil, and prevented the diffusion of water vapor through the straw segments. Also, straw mulching has lower thermal conductivity, which will reduce the quantity of direct solar radiation arriving at the land surface and the magnitudes of the increase in soil temperatures (Horton et al., 1996). Therefore, water in the soil profile is difficult to convert into vapor due to the reduced amount of energy available. All these will consequently reduce the rate of water loss through straw mulching compared with the bare soil. Plastic film, another barrier material, can prevent $E_s$ by blocking the way of water vapor migration to the atmosphere. Crop canopy plays a significant role in reducing $E_s$ (Todd et al., 1991), which was in a good agreement with negative relationship between $E_s$ and LAI found in our study ($r_{ij}$=-0.398, $P_{ij}$<0.001; $b_i$=-0.381, $P_i$<0.001). Raz-Yaseef et al. (2010) indicated that $E_s$ of Yatir ecosystem decreased from 150 to 86 mm $y^{-1}$ from undeveloped canopy cover of 10 % to full canopy closure. Li et al. (2013b) found that merely 20 mm water was lost through soil evaporation in plastic-mulched maize fields due to large canopy shading. Larger shaded under-canopy fraction resulted from higher LAI can also provide another explanation for the decreased $E_s$ with soil mulching in our observations. Declining trend in daily soil evaporation from early to middle stage was also observed, which was primarily due to the variation of LAI. However, unlike other studies conducted in maize fields (Li et al., 2008; Alberto et al., 2014), the senescence of green leaf did not cause the increase in $E_s$ during the late season. This may be attributed to the decrease in solar radiation, $T_a$, VPD and $ET_0$ as well as the increase in RH. Due to the importance of soil evaporation in water loss, many studies have been done to estimate soil evaporation. Kang et al. (2003) reported that seasonal $E_s$ accounted for 26 % of ET of summer maize in three lysimeters in a semi-humid and drought-prone region. Ding et al. (2013b) revealed that $E_s$ of non-mulched maize in Northwest China occupied 31 % of ET, while it only accounted for 14.4 % of ET when plastic film mulching was applied. Our experiments found that $E_s$ averaged over the three growing seasons accounted for 30.11 %, 24.97 %, 16.17 % and 12.59 % of the total ET of summer maize under NM, SM, RPBF and RPSF, respectively, which was generally consistent with previous results.

### *4.3. Plant transpiration*

$T_P$ was the major portion of growing-season ET. The relationship between daily plant transpiration and $ET_0$ was linear since $ET_0$ is a comprehensive meteorological index, which agrees with the findings of

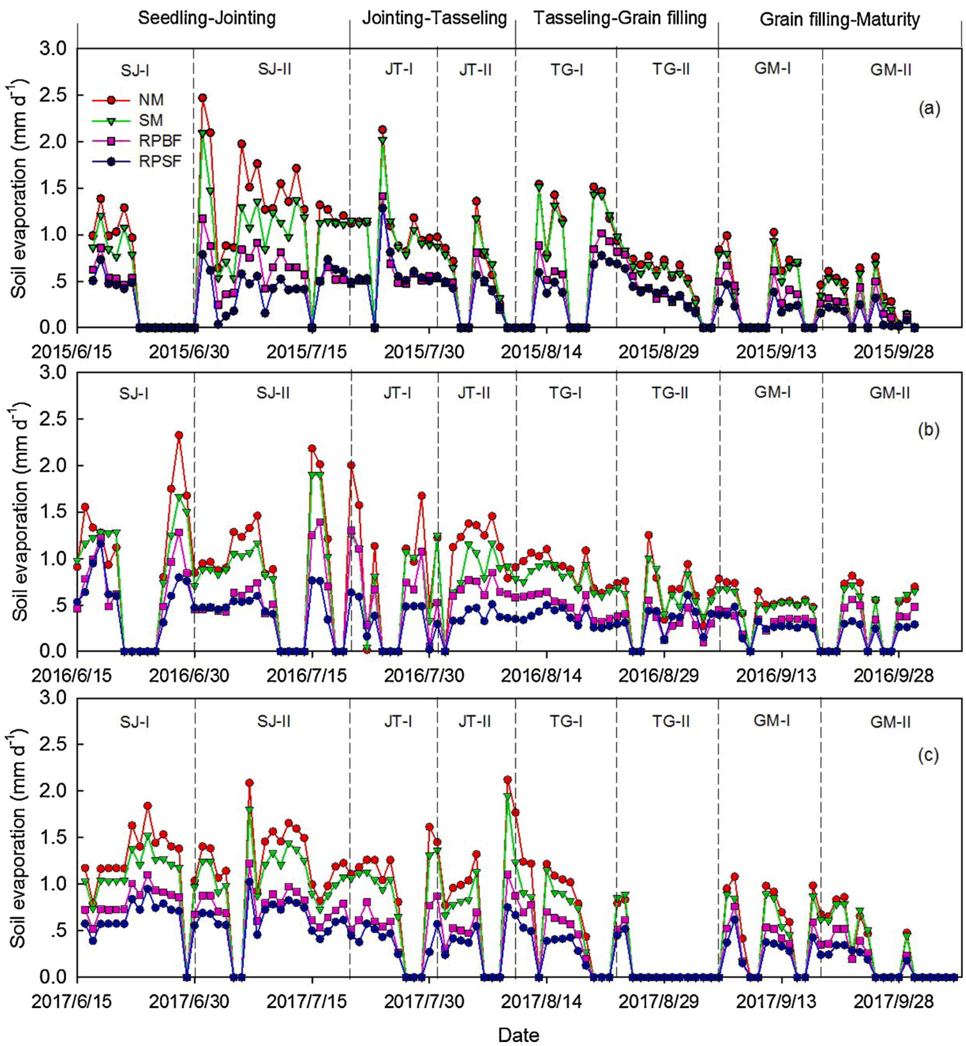


**Fig. 6.** Seasonal variations of soil evaporation of summer maize under various mulching patterns during the study periods of (a) 2015, (b) 2016 and (c) 2017.

Liu et al. (2012) and Jiang et al. (2016). Path analysis showed that $R_s$ was the main meteorological factor controlling $T_P$, with $b_i$ of 0.584, $r_{ij}$ of 0.659 and $R_i^2$ of 0.385. $T_P$ enhanced as $R_s$ increased. Typical diurnal increase-decrease variations of plant transpiration were in accordance to the variation of $R_s$, but lagged around 1 h behind the radiation due to adaption to $R_s$ changes (Zhang et al., 2016). The second factor was $T_a$, with $b_i$ of 0.347, $r_{ij}$ of 0.536 and $R_i^2$ of 0.132. Zhang et al. (2016) and Feng et al. (2017) also pointed out that air temperature had an important influence on plant transpiration. When VPD surpassed a threshold, physiological and transpiration activities of maize were restricted (Oren et al., 2001; Zhou et al., 2004), which resulted in complex responses of $T_P$ to VPD, with positive $r_{ij}$ and $r_{ij}bj$ of 0.517 and 0.603 but negative $b_i$ of -0.086 in our results (Table 2). Among the meteorological variables, the influence of $u_2$ was minimal. The weak relationship between $T_P$ and $u_2$ in our study may result from concentrated wind distribution in the experimental region. In Table 2, $r_{ij}$ of SWC was -0.032, but the influence was not significant ($P_{ij}$>0.05). However, the positive direct action of SWC was extremely significant ($b_i$ = 0.235, $R_i$<0.001). In all, maize plants appeared to reduce stomata opening in leaves and then plant transpiration when SWC dropped below a critical threshold (Guyot et al., 2017). Above this threshold, there was no water stress and plant transpiration mainly depended on atmospheric evaporation demand (Fu et al., 2016). Since $T_P$ is lost primarily through plant stomata, the transpiration rate is closely linked to leaf area (Taiz and Zeigher, 2006). The direct coefficient of LAI was 0.408 and the positive relationship between $T_P$ and LAI has also been demonstrated in previous studies (Liu et al., 2012; Jiang et al., 2016). Enhanced SWC and LAI under straw or plastic film mulching were primarily responsible for the higher plant transpiration when the meteorological conditions were the same as that of non-mulching treatment. At the TG-I stage in 2016, $T_P$ declined dramatically, although measured green LAI at this stage was still high. This can be largely because much less rainfall and higher temperature led to much drier soil conditions, making it difficult for maize roots to absorb soil water and stimulating the production of abscisic acid (ABA)

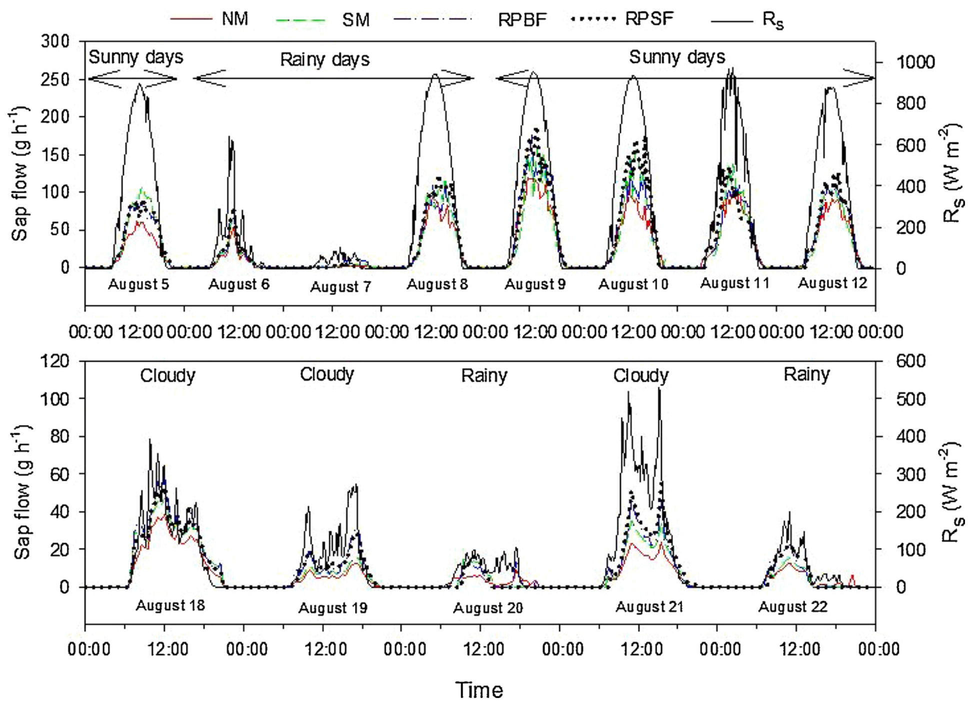


**Fig. 7.** Hourly variations of sap flow rate of summer maize under the four mulching patterns under various weather conditions in 2017.

in the root. Increased ABA can restrict stomatal aperture, which restrains $T_P$ of crops (Zhang et al., 1987). At the TG-II and subsequent growth stages, continuous drought caused leaf drying and yellowing, leading to fast decline in LAI and low level of daily plant transpiration. Alberto et al. (2014) reported that seasonal $T_P$ accounted for 66–74 % of maize ET under overhead sprinkler irrigation. Kang et al. (2003) found that 74.0 % of water was lost by maize transpiration throughout the whole growing season. In general, our observation of seasonal plant transpiration (52.4–73.2 %) was slightly lower or similar to previously published values because maximum maize LAI (3.5-6.2 $m^2$ $m^{-2}$) in our results was lower than or similar to those reported (5.0 or 7.5 $m^2$ $m^{-2}$).

### 4.4. Evapotranspiration

Daily ET was controlled by climatic conditions, such as solar radiation, air temperature, wind speed and relative humidity (Wang and Wang, 2017). Climatic conditions also affect the partitioning of ET, and rainfall was one of the most direct factors influencing sunshine duration and vapor pressure deficit. At each maize growth stage (i.e. SJ-I, SJ-II, JT-I, JT-II, TG-I, TG-II, GM-I and GM-II) in Fig. 10, higher values of $I_c$/ET occurred where greater gross rainfall occurred, which was opposite to the variations of $E_s$/ET. That is to say, $I_c$ accounted for relative larger portion of ET under high rainfall amounts, but relative lower $E_s$/ET would be obtained due to the missing soil evaporation data resulted from the fact that evaporation was theoretically negligible during great rainfall events (>5 mm $day^{-1}$). The partitioning was more influenced by plant growth process, especially plant transpiration. The seasonal variations of $E_s$ and $T_P$ to total ET during the three maize growing seasons were basically in accordance with previous studies (Li et al., 2008; Alberto et al., 2014). It should be acknowledged that there were uncertainties and errors in ET due to the point and touch measurements in this study. For example, micro-lysimeters are unable to measure soil evaporation during rainy days and have constraints in temporal resolution as a result of manual weighing (Kool et al., 2014). Heat-balance sap-flow sensors are subject to errors due to temperature heterogeneity across the plant stem and limited representation of field conditions because of small number of samples (Wang et al., 2017). The collections of throughfall and stemflow may be affected by meteorological factors such as wind speed, leading to biases in canopy interception (Zheng et al., 2018b). However, small relative errors of 9.3–16.1 % over the three growing seasons between $ET_{WB}$ and $ET_{ISP}$ confirmed the satisfactory performances of canopy interception, micro-lysimeter and sap flow measurements to partition ET in our research. In addition, many previous studies also showed that the measurement methods applied in our study can offer convincible evaluation of the three components (Lamm and Manges, 2000; Wang et al., 2007; Zhang et al., 2016).

Growing-season ET of summer maize in our study (237.1–324.4 mm) were close to or smaller than those reported by Yang et al. (2015) in Hunag-Huai-Hai Plain (239.4–552.3 mm) and by Yan et al. (2017) in Guanzhong Plain (299.3–383.0 mm). Different evaporative demand in different years and at different sites may cause these differences. Apart from this, these can be also attributed to the lower rainfall input and lack of irrigation in our study compared to these studies. The difference in total ET among the three seasons was mainly resulted from the maize growth and climatic conditions, particularly the difference in temporal rainfall distribution (Tanaka et al., 2008; Lei and Yang, 2010). Total seasonal ET exhibited no detectable trend under various mulching patterns. The partitioning of canopy interception, soil evaporation and plant transpiration particularly influenced the ultimate ET. When maize plants were small, more soil surface exposed into air, resulting in the increase of soil evaporation under non-mulching. As maize grew, plant transpiration became the dominant component of ET. Also, higher canopy interception with higher leaf area index was observed based on our previous results (Zheng et al., 2018a). All these led to the higher ET under soil mulching at the middle and later maize growth stages. Because the factors influencing canopy interception, soil evaporation and plant transpiration interacted with each other, accumulative ET tended to be irregular throughout the whole growth season. Our results of ET under different mulching patterns were similar to that of Lin et al. (2016), who also observed no significant differences in ET among different mulching treatments.

### 4.5. Grain yield and water productivity

Changing the components of ET is one of the effective approaches for improving crop yield in water-limited areas. Particularly, maximizing

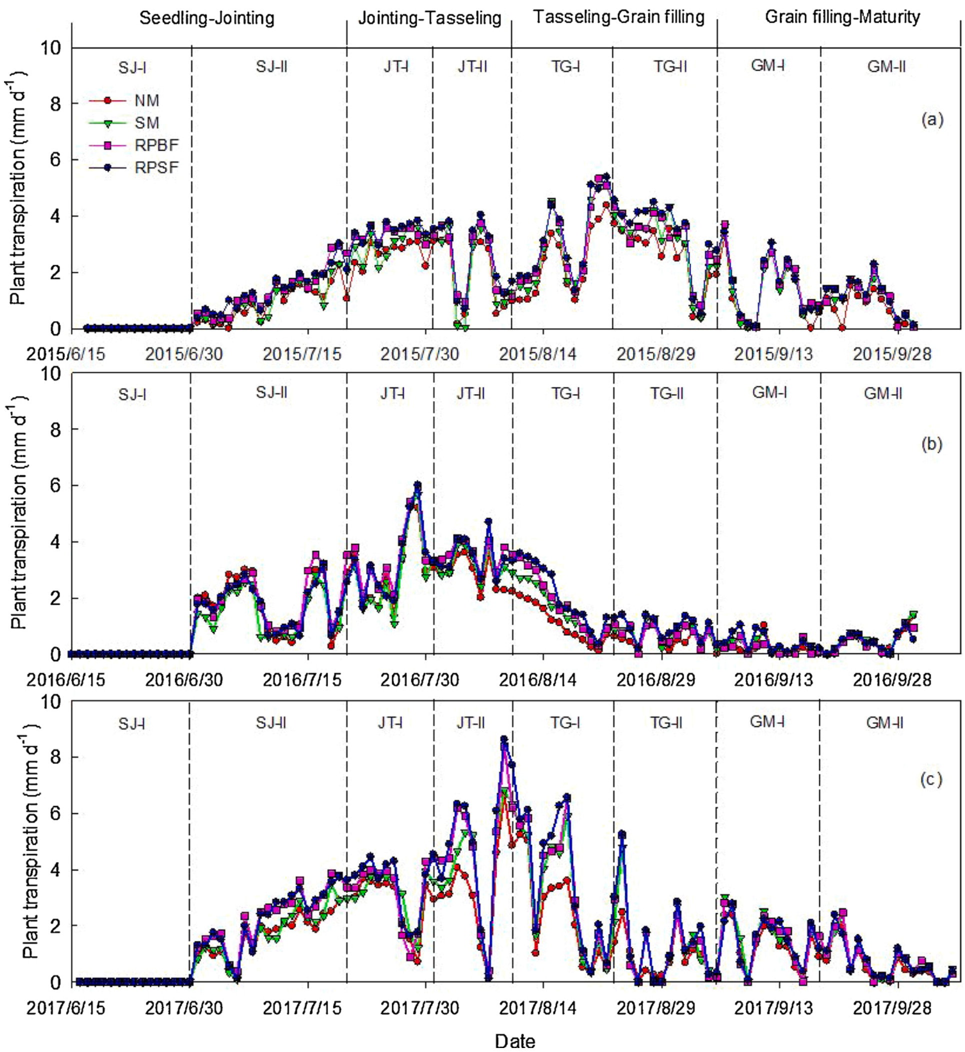


**Fig. 8.** Seasonal variations of daily plant transpiration of summer maize under various mulching patterns during the study periods of (a) 2015, (b) 2016 and (c) 2017.

soil water use for plant transpiration is significant for enhancing WP (Blum, 2009; Rafi et al., 2019). Our results revealed that $I_c$/ET increased from 12.98 to 15.66% under NM to 15.43–17.74 % under RPSF, while $E_s$/ET decreased from 27.60–34.46% to 11.32–15.09 % and $T_P$/ET enhanced from 52.36–58.73% to 65.59–73.24 %. These indicated that soil mulching slightly increased canopy interception loss, but significantly declined the proportion of soil evaporation and improved plant transpiration. Contrasting mulching conditions changed the ways of maize root water uptake by converting more water from unproductive soil evaporation to plant transpiration, which thus increased maize yield and WP.

Many studies have found that straw and plastic film mulching can greatly enhance crop yields (Li et al., 2013a, b), which was in a good agreement with our results (Table 3). In rainfed agriculture, natural rainfall is usually inadequate to meet crop water requirements (e.g., ET) and restricts the grain yield. The growing-season gross rainfall was very similar among the three growth seasons, but their seasonal rainfall distributions differed significantly. Total rainfall in August of 2016 was only 15.7 mm, which was 82.8 % and 80.3 % lower than those in 2015 and 2017, respectively (Fig. 3). Shortage of rainfall at the flowering stage (August 2016) was detrimental to the reproductive development of summer maize (Wang et al., 2011), which explained 60.3 % and 65.0 % lower average yield in 2016 compared with those in 2015 and 2017, respectively. Moreover, average maize yield obtained in 2017 was 13.4 % higher than that in 2015 in our study, which was largely due to 11 % greater rainfall in September 2017 than that in 2015. Abundant soil water during this period could increase the grain-filling rate, grain weight and subsequently enhance maize production (Jia et al., 2018).

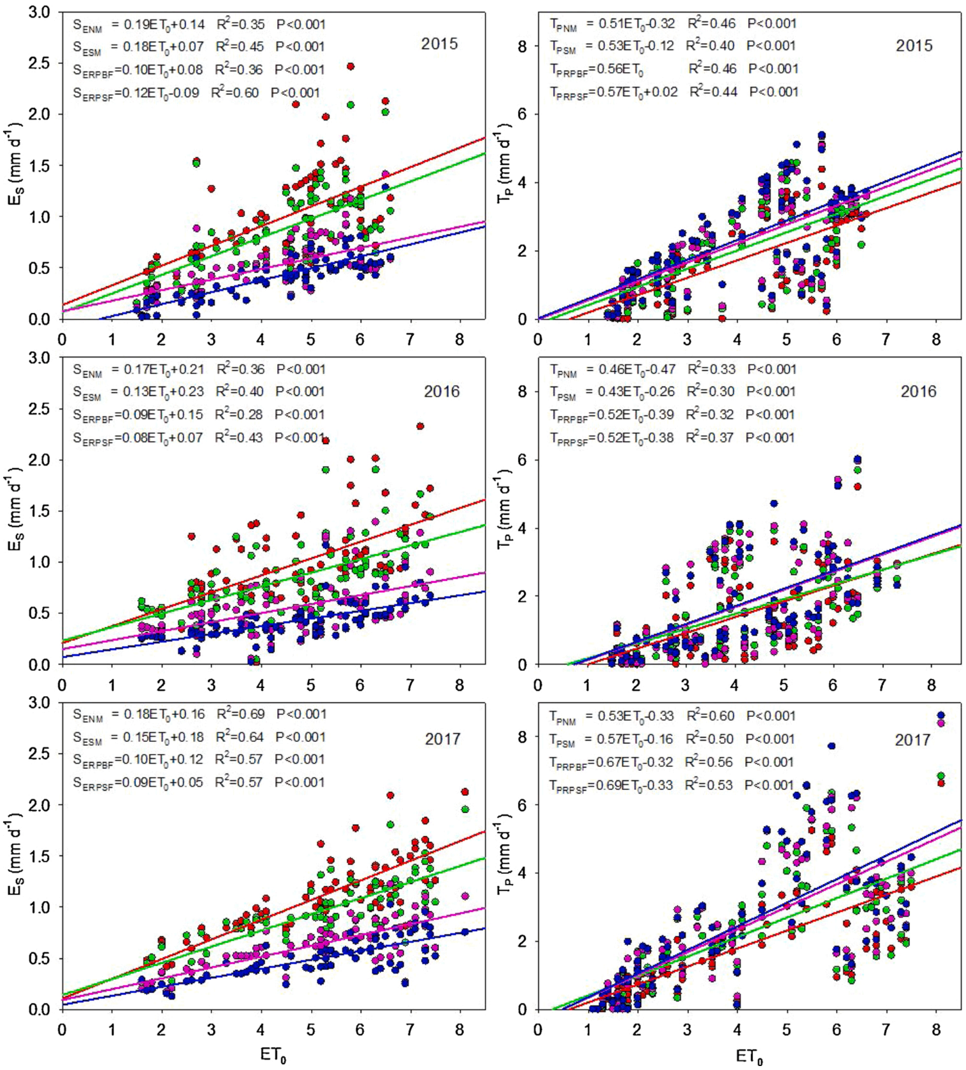


**Fig. 9.** Relationships between daily soil evaporation and plant transpiration under various mulching patterns against $ET_0$ during 2015–2017.

Generally, the distributions of seasonal rainfall in 2015 and 2017 were more uniform than that in 2016. Severe drought occurred during the reproductive period of maize in 2016 better manifested the beneficial effect of ridge-furrow planting for stabling grain yield under extreme climate. Many studies have shown that the effect of this cultivation pattern on crop yield was more obvious when rainfall further decreased. The ridge-furrow mulching system could promote infiltration by collecting rainwater from ridges and conserve more soil water in deep soil to sustain the root-zone soil moisture availability to a certain degree when confronting severe drought (Zhou et al., 2009). Although flat planting with straw mulching has been found to be effective in reducing unproductive evaporation (Lin et al., 2016), it has no promotive effect on rainwater infiltration and even intercepts rainwater to prevent it from infiltrating to the soil, which might cause less available water

**Table 3**
Comparison of grain yield, canopy interception ($I_c$), soil evaporation ($E_s$), plant transpiration ($T_p$), evapotranspiration (ET), and water productivity (WP) of summer maize under various mulching patterns during 2015–2017.

| Year | Treatment | Grain yield (kg $ha^{-1}$) | Total $ET_{ISP}$ (mm) | Total $I_c$ / Total $ET_{ISP}$ (%) | Total $E_s$/ Total $ET_{ISP}$ (%) | Total $T_p$/ Total $ET_{ISP}$ (%) | WP (kg $ha^{-1}$ $mm^{-1}$) | Total $ET_{WB}$ (mm) | Absolute error (mm) | Relative error (%) |
|---|---|---|---|---|---|---|---|---|---|---|
| 2015 | NM | 5936.0b | 264.76a | 12.98a | 28.29a | 58.73b | 22.42b | 241.47a | 23.29 | 9.6 |
| | SM | 6501.3b | 285.73a | 13.18a | 23.17b | 63.65b | 22.75b | 261.47a | 24.27 | 9.3 |
| | RPBF | 7537.3a | 282.42a | 14.69a | 14.29c | 71.02a | 26.69a | 244.95a | 37.48 | 15.3 |
| | RPSF | 7763.0a | 286.64a | 15.43a | 11.32d | 73.24a | 27.08a | 249.37a | 37.27 | 14.9 |
| 2016 | NM | 1366.9b | 241.17a | 13.27b | 34.46a | 52.36b | 5.67b | 213.36a | 27.81 | 13.0 |
| | SM | 1505.4b | 241.93a | 14.45ab | 29.77b | 55.77b | 6.22b | 221.19a | 20.75 | 9.4 |
| | RPBF | 3915.5a | 242.54a | 17.43ab | 19.52c | 63.04a | 16.14a | 210.71a | 31.82 | 15.1 |
| | RPSF | 4232.7a | 237.13a | 19.32a | 15.09d | 65.59a | 17.85a | 204.26a | 32.87 | 16.1 |
| 2017 | NM | 6074.9b | 296.60a | 15.66a | 27.60a | 56.74c | 20.48c | 255.94a | 40.66 | 15.9 |
| | SM | 7662.6ab | 323.17a | 16.01a | 21.97b | 62.02b | 23.71b | 285.15a | 38.02 | 13.3 |
| | RPBF | 8644.5ab | 323.02a | 16.90a | 14.70c | 68.40a | 26.76a | 283.78a | 39.24 | 13.8 |
| | RPSF | 9073.9a | 324.44a | 17.74a | 11.36d | 70.90a | 27.97a | 281.26a | 43.18 | 15.4 |

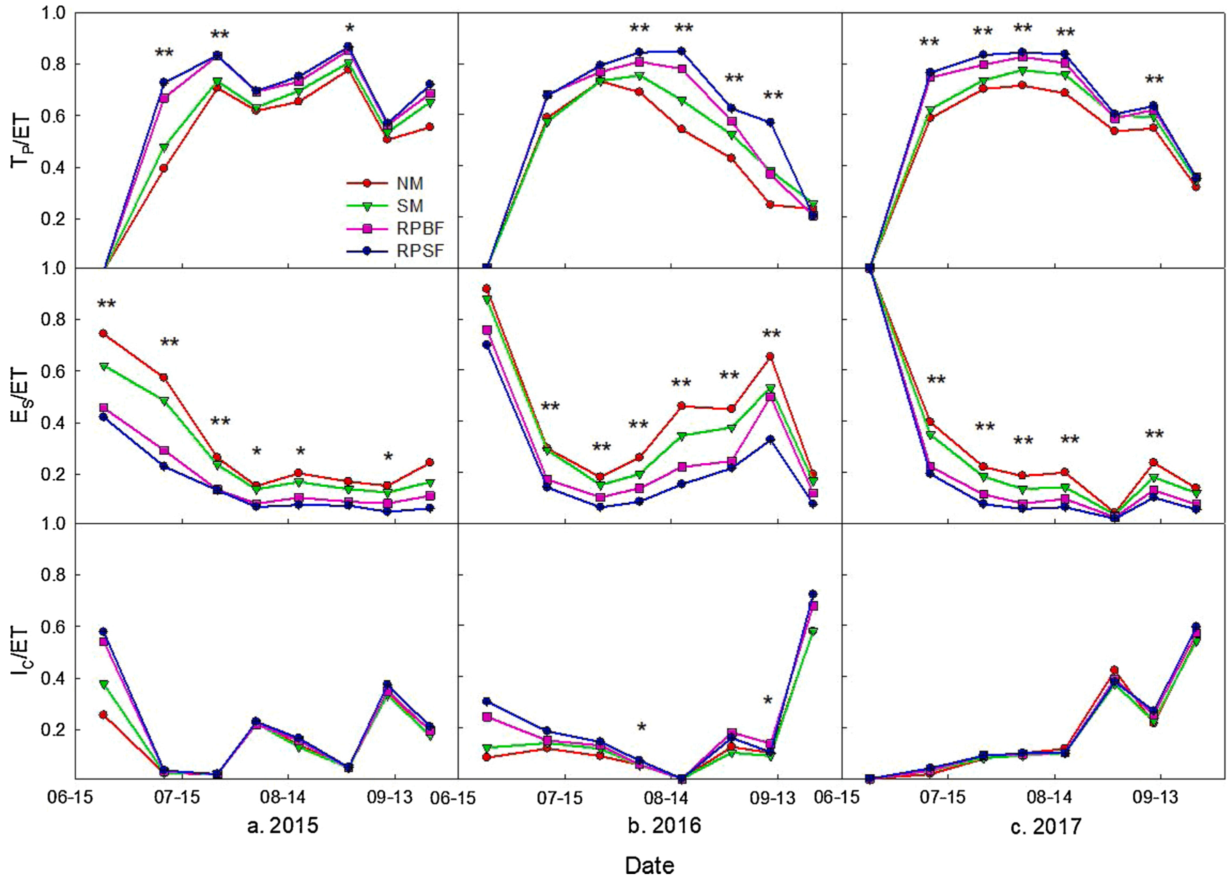


**Fig. 10.** Seasonal variations of $T_p$/ET, $E_s$/ET and $I_c$/ET of summer maize under various mulching patterns during the study periods of 2015–2017.

storage for maize growth in August and thus the much lower increment under SM compared to RPBF and RPSF in 2016. These results indicated that the ridge-furrow planting system was more favorable to maize transpiration and thus the ultimate maize yield and WP. RPSF is more favorable than RPBF resulting from a further decrease in soil evaporation in the furrow while maintaining rainfall-coupled runoff in the furrow. Hu et al. (2019) also concluded that ridge-furrow planting with film mulching on the ridge and wheat straw mulching in the furrow was an effective management practice to increase summer maize yield and WP in the sub-humid but drought-prone region of Northwest China.

## 5. Conclusions

Canopy interception ($I_c$) was an important part of water losses in rainfed agriculture ecosystem, which accounted for 12.3–20.0 % of gross rainfall over the three growing seasons of summer maize during 2015–2017. Soil mulching decreased total $E_s$ by 11.6–56.8 % compared with NM over the three growing seasons. However, seasonal $I_c$ and $T_p$ increased from 32.0–46.4 mm and 126.7–168.3 mm under NM to 44.2–57.6 mm and 155.5–230.0 mm under RPSF, respectively. The ratios of $I_c$, $E_s$ and $T_p$ to total ET also differed under contrasting mulching conditions. $I_c$/ET increased from 12.98–15.66% under NM to 15.43–17.74 % under RPSF, while $E_s$/ET decreased from 27.60–34.46% to 11.32–15.09 % and $T_p$/ET increased from 52.36–58.73% to 65.59–73.24 %. Soil mulching provided more soil water for maize growth by largely decreasing the proportion of soil evaporation even though the loss of canopy interception showed little increase. Relative to NM, grain yield under the three mulching patterns increased by 9.5–30.8 % in 2015, 10.1–209.7 % in 2016 and 26.1–49.4 % in 2017, while WP increased by 1.5–20.8 % in 2015, 9.7–214.8 % in 2016 and 15.8–36.6 % in 2017. Our results are useful for accurately determining ET partitioning and improving the understanding of the mechanism of how contrasting soil mulching patterns make full use of limited rainwater to increase maize yield and water productivity in Northwest China. However, the differences of maize species and site characteristics may also have important impacts on ET partitioning, which have not been explored in the present study. Further studies are thus needed on more maize cultivars across various rainfed regions in Northwest China to verify the results and its application.

## Declaration of Competing Interest

The authors reported no declarations of interest.

## Acknowledgements

This study was jointly supported by the National Natural Science Foundation of China (No. 51879226, 51509208), the Youth Talent Cultivation Program of Northwest A&F University (No. 2452020010) and the “111” Project (B12007). This work was also financially supported by the China Scholarship Council (No. 201906300054) and logistically supported by Purdue University.

## References

Alberto, M.C., Quilty, J.R., Buresh, R.J., Wassmann, R., Haidar, S., Correa, T.Q., Sandro, J.M., 2014. Actual evapotranspiration and dual crop coefficients for dry-seeded rice and hybrid maize grown with overhead sprinkler irrigation. Agric. Water Manage. 136, 1–12.

Allen, R.G., 2011. Skin layer evaporation to account for small precipitation events-An enhancement to the FAO-56 evaporation model. Agric. Water Manage. 99 (1), 8–18.

Allen, R.G., Pereira, L.S., Raes, D., Smith, M., 1998. Crop evapotranspiration-guidelines for computing crop water requirements-FAO Irrigation and Drainage Paper 56, 300 (9). FAO, Rome pp. D05109.

Anapalli, S.S., Ahuja, L.R., Gowda, P.H., Ma, L., Marek, G., Evett, S.R., Howell, T.A., 2016. Simulation of crop evapotranspiration and crop coefficients with data in weighing lysimeters. Agric. Water Manage. 177, 274–283.
Balwinder-Singh, E.H., Gaydon, D.S., Eberbach, P.L., 2016. Evaluation of the effects of mulch on optimum sowing date and irrigation management of zero till wheat in central Punjab, India using APSIM. Field Crops Res. 197, 83–96.
Benyon, R.G., Doody, T.M., 2015. Comparison of interception, forest floor evaporation and transpiration in Pinus radiata and Eucalyptus globulus plantations. Hydrol. Process. 29, 1173–1187.
Blum, A., 2009. Effective use of water (EUW) and not water-use efficiency (WUE) is the target of crop yield improvement under drought stress. Field Crops Res. 112 (2-3), 119–123.
Boast, C.W., Robertson, T.M., 1982. A micro-lysimeter method for determining evaporation from bare soil: description and laboratory evaluation. Soil Sci. Soc. Am. J. 4, 689–696.
Campbell, G.S., Norman, J.M., 1998. Introduction to Environmental Biophysics. Springer Verlag, pp. 286.
Consoli, S., Stagno, F., Vanella, D., Boaga, J., Cassiani, G., Roccuzzo, G., 2017. Partial root-zone drying irrigation in orange orchards: effects on water use and crop production characteristics. Eur. J. Agron. 82, 190–202.
Ding, R., Kang, S., Li, F., Zhang, Y., Tong, L., 2013a. Evapotranspiration measurement and estimation using modified Priestley-Taylor model in an irrigated maize field with mulching. Agric. For. Meteorol. 168, 140–148.
Ding, R., Kang, S., Zhang, Y., Hao, X., Tong, L., Du, T., 2013b. Partitioning evapotranspiration into soil evaporation and transpiration using a modified dual crop coefficient model in irrigated maize field with ground-mulching. Agric. Water Manage. 127, 85–96.
Ding, Z., Li, X., Guo, Y., Leng, X., Wang, M., 2018. Growth and water consumption of maize under degradable mulch in arid sandy area. J. Drain. Irrig. Mach. Eng. 11 (1092), -1097.
Fan, J., Oestergaard, K.T., Guyot, A., Lockington, D.A., 2014. Measuring and modeling rainfall interception losses by a native Banksia woodland and an exotic pine plantation in subtropical coastal Australia. J. Hydrol. 515, 156–165.
Fan, J., Oestergaard, K.T., Guyot, A., Jensen, D.G., Lockington, D.A., 2015. Spatial variability of throughfall and stemflow in an exotic pine plantation of subtropical coastal Australia. Hydrol. Process. 29 (5), 793–804.
Fan, J., Guyot, A., Ostergaard, K.T., Lockington, D.A., 2018. Effects of earlywood and latewood on sap flux density-based transpiration estimates in conifers. Agric. For. Meteorol. 249, 264–274.
Feng, Y., Cui, N., Du, T., Gong, D., Hu, X., Zhao, L., 2017. Ressponse of sap flux and evapotranspiration to deficit irrigation of greenhouse pear-jujube trees in semi-arid northwest China. Agric. Water Manage. 194, 1–12.
Feng, Y., Hao, W., Gao, L., Li, H., Gong, D., Cui, N., 2019. Comparison of maize water consumption at different scales between mulched and non-mulched croplands. Agric. Water Manage. 216, 315–324.
Fu, S., Sun, L., Luo, Y., 2016. Combining sap flow measurements and modelling to assess water needs in an oasis farmland shelterbelt of Populus simonii Carr in Northwest China. Agric. Water Manage. 177, 172–180.
Gong, D., Mei, X., Hao, W., Wang, H., Caylor, K.K., 2017. Comparison of ET partitioning and crop coefficients between partial plastic mulched and non-mulched maize fields. Agric. Water Manage. 181, 23–34.
Gonzalez-Dugo, V., Lopez-Lopez, M., Espadafor, M., Orgaz, F., Testi, L., Zarco-Tejada, P., Fereres, E., 2019. Transpiration from canopy temperature: implications for the assessment of crop yield in almond orchards. Eur. J. Agron. 105, 78–85.
Gu, X., Cai, H., Zhang, Z., Fang, H., Chen, P., Huang, P., Li, Y., Li, Y., Zhang, L., Zhou, H., Du, Y., 2019. Ridge-furrow full film mulching: an adaptive management strategy to reduce irrigation of dryland winter rapeseed (*Brassica napus* L.) in northwest China. Agric. For. Meteorol. 266-267, 119–128.
Guyot, A., Fan, J., Oestergaard, K.T., Whitley, R., Gibbes, B., Arsac, M., Lockington, D.A., 2017. Soil-water content characterisation in a modified Jarvis-Stewart model: a case study of a conifer forest on a shallow unconfined aquifer. J. Hydrol. 544, 242–253.
Han, X., Wang, L., Wang, Y.P., 2014. Canopy interception of summer corn and its influencing factors under natural rainfall. Scientia Agricultural Sinica 47 (8), 1541–1549.
Horton, R., Bristow, K.L., Kluitenberg, G.J., Sauer, T.J., 1996. Crop residue effects on surface radiation and energy balance-review. Theor. Appl. Climatol. 54, 27–37.
Hu, Y., Ma, P., Zhang, B., Hill, R.L., Wu, S., Dong, Q., Chen, G., 2019. Exploring optimal soil mulching for the wheat-maize cropping system in sub-humid drought-prone regions in China. Agric. Water Manage. 219, 59–71.
Huang, G., Chen, W., Li, F., 2011. Rainfed farming systems in the loess plateauof China. In: Tow, P., Cooper, I., Partridge, I., Birch, C. (Eds.), Rainfed FarmingSystems. Springer, Netherlands, pp. 643–669.
Jia, Q., Sun, L., Mou, H., Shahzad, A., Liu, D., Zhang, Y., Zhang, P., Ren, X., Jia, Z., 2018. Effects of planting patterns and sowing densities on grain-filling, radiation use efficiency and yield of maize (Zea mays L.) in semi-arid regions. Agric. Water Manage. 201, 287–298.
Jiang, X., Kang, S., Li, F., Du, T., Tong, L., Comas, L., 2016. Evapotranspiration partitioning and variation of sap flow in female and male parents of maize for hybrid seed production in arid region. Agric. Water Manage. 176, 132–141.
Kang, S., Gu, B., Du, T., Zhang, J., 2003. Crop coefficient and ratio of transpiration to evapotranspiration of winter wheat and maize in a semi-humid region. Agric. Water Manage. 59 (3), 239–254.
Kool, D., Agam, N., Lazarovitch, N., Heitman, J.L., Sauer, T.J., Ben-Gal, A., 2014. A review of approaches for evapotranspiration partitioning. Agric. For. Meteorol. 184, 56–70.
Kraus, J.H., 1966. Application efficiency of sprinkler irrigation and its effects on microclimate. Trans. ASAE 9, 642–645.
Lamm, F.R., Manges, H.L., 2000. Partitioning of sprinkler irrigation water by a corn canopy. Trans. ASAE 43 (4), 909–918.
Lei, H., Yang, D., 2010. Interannual and seasonal variability in evapotranspiration and energy partitioning over an irrigated cropland in the North China Plain. Agric. For. Meteorol. 150, 581–589.
Li, S., Kang, S., Li, F., Zhang, L., 2008. Evapotranspiration and crop coefficient of spring maize with plastic mulch using eddy covariance in northwest China. Agric. Water Manage. 95 (11), 1214–1222.
Li, C., Ren, D., Wang, G., Hu, H., Li, T., Liu, G., 2009. Analysis of artificial precipitation interception over two meadow species on Qinghai-Tibet plateau. Adv. Water Sci. 20 (6), 769–774.
Li, R., Hou, X., Jia, Z., Han, Q., Ren, X., Yang, B., 2013a. Effects on soil temperature, moisture, and maize yield of cultivation with ridge and furrow mulching in the rainfed area of the Loess Plateau. China. Agric. Water Manage. 116, 101–109.
Li, S., Wang, Z., Li, S., Gao, Y., TIan, X., 2013b. Effect of plastic sheet mulch, wheat straw mulch, and maize growth on water loss by evaporation in dryland areas of China. Agric. Water Manage. 116, 39–49.
Li, X., Šimůnek, J., Shi, H., Yan, J., Peng, Z., Gong, X., 2017. Spatial distribution of soil water, soil temperature, and plant roots in a drip-irrigated intercropping field with plastic mulch. Eur. J. Agron. 83, 47–56.
Li, S., Li, Y., Lin, H., Feng, H., Dyck, M., 2018. Effects of different mulching technologies on evapotranspiration and summer maize growth. Agric. Water Manage. 201, 309–318.
Lin, D., Zheng, Z., Zhang, X., 2011. Study on the effect of maize plants onrainfall redistribution processes. Sci. Agric. Sin. 44 (12), 2608–2615.
Lin, W., Liu, W.Z., Xue, Q., 2016. Spring maize yield, soil water use and water use efficiency under plastic film and straw mulches in the Loess Plateau. Sci. Rep. 6, 1–10.
Liu, C., Du, T., Li, F., Kang, S., Li, S., Tong, L., 2012. Trunk sap flow characteristics during two growth stages of apple tree and its relationships with affecting factors in an arid region of northwest China. Agric. Water Manage. 104, 193–202.
Liu, X., Li, X., Guo, R., Kuzyakov, Y., Li, F., 2015. The effect of plastic mulch on the fate of urea-N in rain-fed maize production in a semiarid environment as assessed by 15N-labeling. Eur. J. Agron. 70, 71–77.
Liu, Z., Zhu, K., Dong, S., Liu, P., Zhao, B., Zhang, J., 2017. Effects of integrated agronomic practices management on root growth and development of summer maize. Eur. J. Agron. 84, 140–151.
Liu, M., Shi, H., Li, X., Yan, J., Sun, W., Dou, X., 2018. Path analysis of evapotranspiration dynamic variation and its influencing factors in Hetao Irrigation District. J. Drain. Irrig. Mach. Eng. 11, 1086.
Mckee, G.W., 1964. A coefficient for computing leaf area in hybrid corn. Agron. J. 56, 240–241.
Mo, F., Li, X.Y., Niu, F.J., Zhang, C., Li, S., Zhang, L., Xiong, Y., 2018. Alternating small and large ridges with full film mulching increase linseed (Linum usitatissimum L.) productivity and economic benefit in a rainfed semiarid environment. Field Crops Res. 219, 120–130.
Monteith, J., 1981. Evapotranspiration and surface temperature. Q. J. R. Meteorol. Soc. 107 (451), 1–27.
Oren, R., Sperry, J.S., Ewers, B.E., Pataki, D.E., Phillips, N., Megonigal, J.P., 2001. Sensitivity of mean canopy stomatal conductance to vapor pressure deficit in a flooded Taxodium distichum L. forest: hydraulic and non-hydraulic effects. Oecologia 126 (1), 21–29.
Penman, H.L., 1948. Natural Evapotranspiration From Open Water, Bare Soil and Grass. The Royal Society, pp. 120–145.
Rafi, Z., Merlin, O., Dantec, V.L., Khabba, S., Mordelet, P., Er-Raki, S., Amazirh, A., Olivera-Guerra, L., Hssaine, B.A., Simonneaux, V., Ezzahar, J., Ferrer, F., 2019. Partitioning evapotranspiration of a drip-irrigated wheat crop: intercomparing eddy covariance, sap flow, lysimeter and FAO-based methods. Agric. For. Meteorol. 265, 310–326.
Raz-Yaseef, N., Rotenberg, E., Yakir, D., 2010. Effects of spatial variations in soil evaporation caused by tree shading on water flux partitioning in a semi-arid pine forest. Agric. For. Meteorol. 150 (3), 454–462.
Raz-Yaseef, N., Yakir, D., Schiller, G., Cohen, S., 2012. Dynamics of evapotranspiration partitioning in a semi-arid forest as affected by temporal rainfall patterns. Agric. For. Meteorol. 157, 77–85.
Stewart, J.B., 1977. Evapotranspiration from the wet canopy of a pine forest. Water Resour. Res. 13 (6), 915–921.
Taiz, L., Zeigher, E., 2006. Plant Physiology, 4th ed. Sinauer Associate, Inc, Publisher, Sunderland, Massachusetts.
Tanaka, K., Takizawa, H., Shiraki, K., Tantasirin, C., Tangtham, N., Suzuki, M., 2008. A review of evapotranspiration estimates from tropical forests in Thailand and adjacent regions. Agric. For. Meteorol. 148 (5), 807–819.
Todd, R.W., Klocke, N.L., Hergert, G.W., Parkhurst, A.M., 1991. Evaporation from soil influenced by crop shading, crop residue, and wetting regime. Trans. ASAE 34, 461–466.
Wang, H., Liu, C., 2007. Soil evaporation and its affection factors under crop canopy. Commun. Soil Sci. Plant Anal. 38, 259–271.
Wang, D., Wang, L., 2017. Dynamics of evapotranspiration partitioning for apple trees of different ages in a semiarid region of northern China. Agric. Water Manage. 191, 1–15.
Wang, X., Fan, J., Xing, Y., Xu, G., Wang, H., Deng, J., Wang, Y., Zhang, F., Li, P., Li, Z., 2019a. The effects of mulch and nitrogen fertilizer on the soil environment of crop plants. Adv. Agron. 153, 121–173.

Wang, D., Li, J.S., Rao, M.J., 2007. Field evaluating the effect of microclimate modification resulted from sprinkler irrigation on crop transpiration. J. Hydraul. Eng. 38 (4), 427–433.
Wang, T., Wei, L., Wang, H., Ma, S., Ma, B., 2011. Responses of rainwater conservation, precipitation-use efficiency and grain yield of summer maize to a furrow-planting and straw-mulching system in northern China. Field Crops Res. 124, 223–230.
Wang, Y., Zhang, X., Xiao, X., Heitman, J., Horton, R., Ren, T., 2017. An empirical calibration for heat-balance sap-flow sensors in maize. Agronomy 109 (3), 1122–1128.
Wang, P., Deng, Y., Li, X., Wei, Z., Hu, X., Tian, F., Wu, X., Huang, Y., Ma, Y., Zhang, C., Wang, Y., Li, E., Wang, J., 2019b. Dynamical effects of plastic mulch on evapotranspiration partitioning in a mulched agriculture ecosystem: measurement with numerical modeling. Agric. For. Meteorol. 268, 98–108.
Yan, W., Chen, S., Tian, D., Kang, W., 2005. Contribution of cinnamomum camphora (L.) presl plantation to precipitation redistributin. Bull. Soil Water Conserv. 25 (6), 10–13.
Yan, S., Zhang, F., Wu, Y., Qiang, S., Zou, H., Xiang, Y., Fan, J., Tian, J., 2017. Estimation of drip irrigated summer maize soil water content and evapotranspiration based on SIMDualKc model. Trans. CSAE 33 (16), 152–160.
Yang, J., Mei, X., Huo, Z., Yan, C., Ju, H., Zhao, F., Liu, Q., 2015. Water consumption in summer maize and winter wheat cropping system based on SEBAL model in Huang-Huai-Hai Plain, China. J. Integr. Agr. 14 (10), 2065–2076.
Yimam, Y.T., Ochsner, T.E., Kakani, V.G., 2015. Evapotranspiration partitioning and water use efficiency of swichgrass and biomass sorghum managed for biofuel. Agric. Water Manage. 155, 40–47.
Zhang, J., Schum, U., Davies, W.J., 1987. Control of stomatal behavior by abscisic acid which apparently originates in roots. J. Exp. Bot. 38, 1174–1181.
Zhang, Y., Kang, S., Ward, E.J., Ding, R., Zhang, X., Zheng, R., 2011. Evapotranspiration components determined by sap flow and microlysimetry techniques of a vineyard in northwest China: dynamics and influential factors. Agric. Water Manage. 98 (8), 1207–1214.
Zhang, Y., Wang, X., Hu, R., Pan, Y., Paradeloc, M., 2015. Rainfall partitioning into throughfall, stemflow and interception loss by two xerophytic shrubs within a rain-fed re-vegetated desert ecosystem, northwestern China. J. Hydrol. 527, 1084–1095.
Zhang, B., Xu, D., Liu, Y., Li, F., Cai, J., Du, L., 2016. Multi-scale evapotranspiration of summer maize and the controlling meteorological factors in north China. Agric. For. Meteorol. 216, 1–12.
Zheng, J., Fan, J., Zou, Y., Chau, H.W., Zhang, F., 2020. Ridge-furrow plastic mulching with a suitable planting density enhances rainwater productivity, grain yield and economic benefit of rainfed maize. J. Arid Land 12, 181–198.
Zheng, Z., Li, T., Zhang, X., Wang, Y., Lin, C., 2012. Differentiation characteristics and influencing factors of rainfall interception in maize plants. J. Soil Water Conserv. 26 (4), 208–211.
Zheng, J., Fan, J., Zhang, F., Yan, S., Guo, J., Chen, D., Li, Z., 2018a. Mulching mode and planting density affect canopy interception loss of rainfall and water use efficiency of dryland maize on the Loess Plateau of China. J. Arid Land 10 (5), 794–808.
Zheng, J., Fan, J., Zhang, F., Yan, S., Xiang, Y., 2018b. Rainfall partitioning into throughfall, stemflow and interception loss by maize canopy on the semi-arid Loess Plateau of China. Agric. Water Manage. 195, 25–36.
Zheng, J., Fan, J., Zhang, F., Yan, S., Wu, Y., Lu, J., Guo, J., Cheng, M., Pei, Y., 2019. Throughfall and stemflow heterogeneity under the maize canopy and its effect on soil water distribution at the row scale. Sci. Total Environ. 660, 1367–1382.
Zhou, H., Li, X., Fan, H., Wang, X., Tan, H., Li, A., 2004. Physiological characteristics of several Caragana shrub species under extreme conditions. J. Desert Res. 25, 182–190.
Zhou, L., Li, F., Jin, S., Song, Y., 2009. How two ridges and the furrow mulched with plastic film affect soil water, soil temperature and yield of maize on the semiarid Loess Plateau of China. Field Crops Res. 113, 41–47.